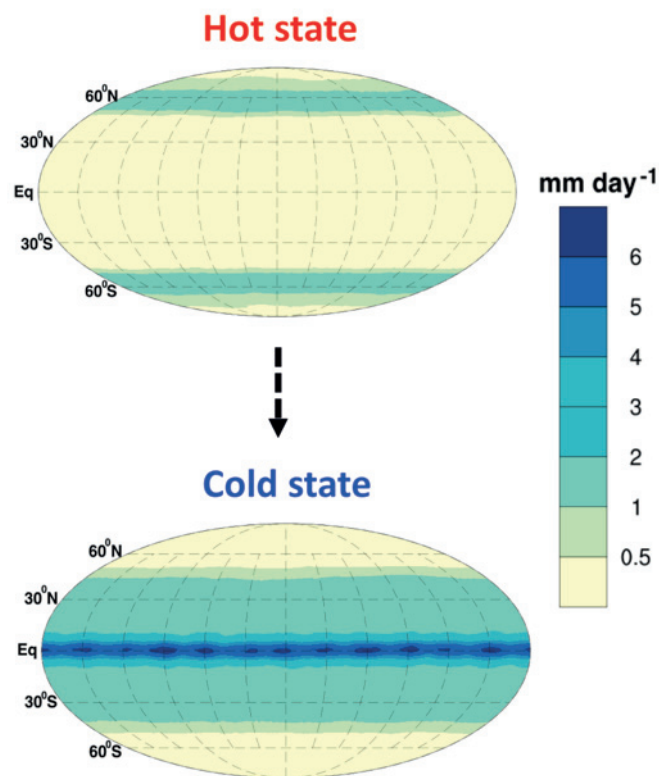


## Multiple climate states and bifurcations on Earth-like terra-planets



Sirisha Kalidindi

Hamburg 2019

## Hinweis

Die Berichte zur Erdsystemforschung werden vom Max-Planck-Institut für Meteorologie in Hamburg in unregelmäßiger Abfolge herausgegeben.

Sie enthalten wissenschaftliche und technische Beiträge, inklusive Dissertationen.

Die Beiträge geben nicht notwendigerweise die Auffassung des Instituts wieder.

Die "Berichte zur Erdsystemforschung" führen die vorherigen Reihen "Reports" und "Examensarbeiten" weiter.

## Anschrift / Address

Max-Planck-Institut für Meteorologie  
Bundesstrasse 53  
20146 Hamburg  
Deutschland

Tel./Phone: +49 (0)40 4 11 73 - 0  
Fax: +49 (0)40 4 11 73 - 298

name.surname@mpimet.mpg.de  
www.mpimet.mpg.de

## Notice

The Reports on Earth System Science are published by the Max Planck Institute for Meteorology in Hamburg. They appear in irregular intervals.

They contain scientific and technical contributions, including Ph. D. theses.

The Reports do not necessarily reflect the opinion of the Institute.

The "Reports on Earth System Science" continue the former "Reports" and "Examensarbeiten" of the Max Planck Institute.

## Layout

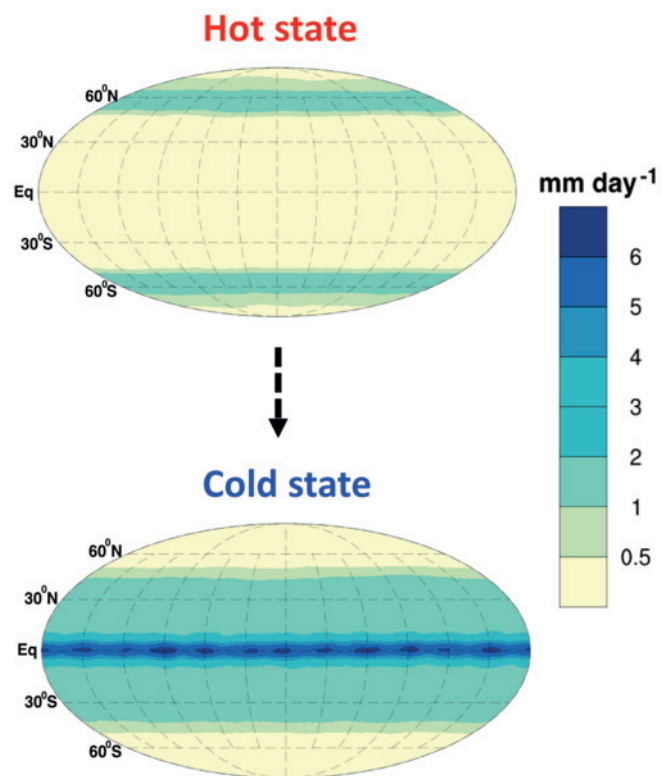
Bettina Diallo and Norbert P. Noreiks  
Communication

## Copyright

Photos below: ©MPI-M  
Photos on the back from left to right:  
Christian Klepp, Jochem Marotzke,  
Christian Klepp, Clotilde Dubois,  
Christian Klepp, Katsumasa Tanaka



# Multiple climate states and bifurcations on Earth-like terra-planets



Sirisha Kalidindi

Hamburg 2019

# Sirisha Kalidindi

from Tadepalligudem, India

Max-Planck-Institut für Meteorologie  
The International Max Planck Research School on Earth System Modelling  
(IMPRS-ESM)  
Bundesstrasse 53  
20146 Hamburg

Universität Hamburg  
Geowissenschaften  
Meteorologisches Institut  
Bundesstr. 55  
20146 Hamburg

Tag der Disputation: 5. April 2019

Folgende Gutachter empfehlen die Annahme der Dissertation:

Dr. Christian Reick  
Prof. Dr. Martin Claussen

Vorsitzender des Promotionsausschusses:

Prof. Dr. Dirk Gajewski

Dekan der MIN-Fakultät:

Prof. Dr. Heinrich Graener

# Abstract

Past studies have shown that terra-planets (land planets with limited water inventories) support a dry climate with all the water on the planet trapped at high latitudes in ice caps [Abe et al., 2005, 2011]. Whether such dry planets can maintain surface liquid water to promote life is unclear. Leconte et al. (2013) argue that on terra-planets, mechanisms like gravity driven ice flows and geothermal flux can maintain liquid water at the edges and bottom of ice caps. This water may then flow back to lower latitudes in rivers or subsurface flows. However, none of the past studies on Earth-like terra-planets have accounted for such an overland water recycling mechanism. Here, I analyse the influence of water recycling on the climate of Earth-like terra-planets using the state of the art general circulation model ICON equipped with an efficient overland water recycling mechanism.

For such a planet I find two drastically different climate states for the same boundary conditions: a hot and dry (HD) state with only high-latitude precipitation that was reported by past studies and an additional climate state – a cold and wet (CW) state with dominant low-latitude precipitation. For perpetual equinox conditions, both the climate states are stable below a certain threshold value of soil surface albedo indicating climate bistability while above the threshold only the CW state is stable.

Rocky planets like Earth with liquid water on the surface may undergo a drastic climate shift either towards a completely ice covered state (Snowball state) or towards a very hot moist greenhouse state by evaporation of all water bodies on the planet. In this thesis, I demonstrate that in addition to these two well-known climate instabilities, Earth-like terra-planets can undergo a new type of abrupt climate shift from the HD state to the CW state in the presence of an effective overland water recycling mechanism. I refer to this new climate instability as the ‘terra-planet bifurcation’. The terra-planet bifurcation occurs when the soil surface albedo in the HD state is increased above a threshold value and is associated with a cooling of about 35° C globally, which is of the order of the temperature difference between present day Earth and the Snowball Earth state. While the Snowball and the moist greenhouse bifurcations are forced by radiative feedbacks, I find that the terra-planet bifurcation is triggered by local hydrological feedbacks.

Starting from the CW state and reversing the forcing, i.e. reducing the soil surface albedo to zero, does not shift back the terra-planet to the HD state which indicates hysteretic behaviour. But, the hysteretic loop is not closed. Mechanisms leading to the terra-planet bistability and the hysteretic behaviour are discussed in this thesis and complete evaporation of rain drops is identified as the key process.

Additionally, I illustrate that bistability in climate on Earth-like terra-planets is strongly influenced by obliquity. The width of the bi-stable region (range of soil surface albedo values for

which both the HD and CW climate states are stable) is significantly reduced with the increase in obliquity. And for present-day Earth's obliquity, the terra-planet exhibits mono-stability – only the CW state exists. For obliquities of 5° and 7°, an additional climate bifurcation occurs. This climate bifurcation is similar to the terra-planet bifurcation but the resulting climate is hot and wet (HW) characterised by intense precipitation in the low-latitude region and warmer temperatures compared to the CW state.

Overall my findings reveal that for a wide range of parameter values, liquid water can exist on Earth-like terra-planets, provided a recycling mechanism exists which can transport water from the high latitudes back to the low latitudes. Moreover, the hydrology on such planets can be very unstable and hydrological feedbacks can lead to drastically different hydro-climate states.

# Zusammenfassung

Frühere Studien haben gezeigt, dass Terraplaneten (Landplaneten mit begrenzten Wasservorkommen) ein trockenes Klima aufrechterhalten, da das gesamte Wasser auf dem Planeten in hohen Breitengraden in Eiskappen gespeichert ist [Abe et al., 2005, 2011]. Es ist unklar, ob derartige trockene Planeten Wasser in flüssiger Form an der Oberfläche aufweisen können, um Leben zu ermöglichen. Leconte et al. (2013) argumentieren, dass auf Terraplaneten durch schwerkraftgetriebene Eisströme und geothermischen Fluss Wasser im flüssigen Aggregatzustand an den Rändern und am Boden von Eiskappen existieren kann. Dieses Wasser könnte dann in Flüssen oder unterirdisch in Richtung des Äquators zurückfließen. Keine der bisherigen Studien hat jedoch auf erdähnlichen Terraplaneten einen solchen Mechanismus für einen unter- und überirdischen Rückfluss von Wasser berücksichtigt. Deswegen analysiere ich den Einfluss dieses äquatorial gerichteten

Wassertransportes auf das Klima erdähnlicher Terraplaneten mit dem hochmodernen atmosphärischen Zirkulationsmodell ICON, welches in der Lage ist, diesen Rücktransport von Wasser in Richtung des Äquators im Boden und an der Erdoberfläche zu simulieren.

Für einen solchen Planeten finde ich zwei drastisch unterschiedliche Klimazustände für die gleichen Randbedingungen: einen heißen und trockenen (HD) Zustand mit Niederschlägen nur in den hohen Breiten, wie sie in früheren Studien bereits berichtet wurden, und einen zusätzlichen Klimazustand - einen kalten und nassen (CW) Zustand mit Niederschlägen, die in den niederen Breiten dominieren. Unter Bedingungen permanenter Tagundnachtgleiche sind beide Klimazustände unterhalb eines bestimmten Schwellenwerts der Bodenoberflächenalbedo stabil, was auf eine Bistabilität im Klima hinweist, während oberhalb dieses Schwellenwerts nur der CW-Zustand stabil ist.

Es ist bekannt, dass Gesteinsplaneten wie die Erde mit flüssigem Wasser an der Oberfläche eine drastische Klimaänderung durchlaufen können, entweder in Richtung eines vollständig eisbedeckten Zustands (Schneeball-Erde) oder in Richtung eines sehr heißen, feuchten Zustands (Treibhaus-Erde) durch Verdunstung aller Gewässer auf dem Planeten. In dieser Arbeit zeige ich, dass zusätzlich zu diesen beiden bekannten Klimainstabilitäten erdähnliche Terraplaneten eine neue Art von abruptem Klimawechsel vom HD-Zustand in den CW-Zustand durchlaufen können, falls ein Wassertransport im Boden und an der Erdoberfläche vorhanden ist. Ich bezeichne diese neue Klimainstabilität als die "Terraplanet-Bifurkation". Die "Terraplanet-Bifurkation" tritt auf, wenn die Bodenoberflächenalbedo im HD-Zustand über einen bestimmten Schwellenwert erhöht wird. Sie ist mit einer globalen Abkühlung von etwa 35° C verbunden, was in der Größenordnung der Temperaturdifferenz zwischen dem heutigen Erdklima und dem Zustand der „Schneeball-Erde“ liegt. Während die Zustände der sogenannten „Schneeball-Erde“ und der feuchten „Treibhaus-Erde“ von Strahlungsrückwirkungen hervorgerufen werden, wird die "Terraplanet-Bifurkation" durch lokale hydrologische Rückkopplungen ausgelöst.

Befindet sich der Terraplanet im CW-Zustand, so führt eine Umkehrung der Richtung der Antriebsänderungen, d.h. die Reduktion der Bodenoberflächenalbedowerte auf Null, den Terraplaneten nicht zurück in den HD-Zustand. Dieses deutet auf ein hysteretisches Verhalten hin. Aber der Hysterese ist nicht geschlossen. Mechanismen, die zur Bistabilität des Terraplaneten und zum hysteretischen Verhalten führen, werden in meiner Arbeit diskutiert. Insbesondere zeige ich, dass die vollständige Verdunstung von Regentropfen ein Schlüsselprozess sowohl für die Bistabilität als auch für das hysteretische Verhalten ist.

Darüber hinaus veranschauliche ich, dass die Bistabilität des Klimas auf erdähnlichen Terraplaneten stark von der Schiefe der Rotationsachse beeinflusst wird. Die Breite des bistabilen Bereichs (Wertebereich der Bodenoberflächenalbedowerte für den sowohl der HD- als auch der CW-Klimazustand stabil sind) wird mit zunehmender Schiefe der Ekliptik deutlich reduziert. Für Werte der heutigen Erdneigung zeigt der Terraplanet Monostabilität - nur der CW-Zustand existiert. Es gibt eine zusätzliche Bifurkation für die Schrägen  $5^\circ$  und  $7^\circ$ . Diese Bifurkation ist ähnlich wie die Terraplanten-Bifurkation, aber das resultierende Klima ist warm und nass (HW), insbesondere ist es durch intensive Niederschläge in den niederen Breiten und wärmere Temperaturen im Vergleich zum CW-Zustand gekennzeichnet.

Insgesamt zeigen meine Ergebnisse, dass für eine Vielzahl von Parameterwerten flüssiges Wasser auf erdähnlichen Terraplaneten existieren kann, vorausgesetzt, es existiert ein Transportmechanismus, der Wasser aus den hohen Breiten in die niederen Breiten zurückführen kann. Darüber hinaus kann die Hydrologie auf solchen Planeten sehr instabil sein und eine Kombination von hydrologischen und Wolken-Rückkopplungseffekten kann zu drastisch unterschiedlichen Hydroklimazuständen führen.

## **TEILVERÖFFENTLICHUNGEN DIESER DISSERTATION**

### **Pre-published work related to this dissertation**

Kalidindi, S., Reick, C. H., Raddatz, T., and Claussen, M. (2018): Two drastically different climate states on an Earth-like terra-planet, *Earth Syst. Dynam.*, 9, 739-756, <https://doi.org/10.5194/esd-9-739-2018>.

# CONTENTS

---

Abstract.....	III
Zusammenfassung.....	V
List of Tables.....	X
List of Figures.....	XI
Abbreviations.....	XIII
<b>1 Introduction.....</b>	<b>15</b>
1.1 Background.....	15
1.2 Past studies on terra-planets.....	16
1.3 Multiple climate states.....	18
1.4 The effect of obliquity on the climate of terra-planets.....	18
1.5 Thesis Outline.....	19
<b>2 Model and Simulation Setup.....</b>	<b>21</b>
2.1 Model.....	21
2.2 Terra-planet configuration.....	21
2.3 Simulations.....	23
2.4 Sequence of simulations that led to the discovery of the terra-planet bi-stability.....	24
<b>3 Drastically different climate states for perpetual equinox.....</b>	<b>27</b>
3.1 Mean climate.....	27
3.1.1 Surface temperature.....	27
3.1.2 Precipitation.....	28
3.1.3 Feedbacks that keep the HD state dry and the CW state wet.....	29
3.1.4 Feedbacks that keep the HD state hot and CW state cold.....	30
3.1.5 Mean circulation and energy transport.....	30
3.2 Transition to the CW state.....	33
3.3 Hysteresis.....	35
3.4 Does snow albedo feedback play a role in the emergence of the two climate states?.....	36
3.5 Discussion and conclusions.....	37
<b>4 Mechanisms behind the planetary scale climate bifurcation on Earth like Terra planets ...</b>	<b>41</b>
4.1 Revisiting the terra-planet bifurcation identified in chapter 3.....	41
4.2 Characteristics of the Terra-planet bifurcation.....	43
4.3 Stability of the HD state.....	46
4.4 Transition from the HD state to the CW state.....	47
4.5 Stability of the CW state.....	51

4.6	Summary .....	52
<b>5</b>	<b>The Effect of obliquity on the climate of terra-planets .....</b>	<b>55</b>
5.1	Three drastically different climate states with non-zero obliquity .....	55
5.2	Mean climate of the Hot and Wet (HW) state .....	56
5.3	Two different climate instabilities with non-zero obliquity .....	59
5.3.1	Abrupt transition from HD state to CW state .....	59
5.3.2	Abrupt transition from HD state to HW state .....	60
5.3.3	Gradual transition from HW state to CW state .....	60
5.4	Bistability and hysteresis with non-zero obliquity .....	60
5.5	No bistability or hysteresis for $\varnothing=5^\circ$ .....	61
5.6	Discussion and Conclusions .....	62
<b>6</b>	<b>Conclusions and Outlook.....</b>	<b>65</b>
6.1	Conclusions .....	65
6.2	Outlook .....	67
	<b>Bibliography.....</b>	<b>71</b>
	<b>Acknowledgements.....</b>	<b>76</b>

# List of tables

<b>Table 2.1</b> Summary of simulations performed in this study.....	<b>24</b>
<b>Table 2.2</b> Summary of simulations performed to illustrate the procedure followed by which I found bistability on my terra-planet.....	<b>25</b>

# List of figures

<b>Figure 2.1 (a)</b> Time series of global mean surface temperature ( $^{\circ}\text{C}$ ) and <b>(b)</b> annual mean meridional profile of precipitation ( $\text{mm day}^{-1}$ ).....	<b>25</b>
<b>Figure 3.1</b> Time series of global mean surface temperature ( $^{\circ}\text{C}$ ) and precipitation ( $\text{mm day}^{-1}$ ).....	<b>27</b>
<b>Figure 3.2</b> Annual mean meridional profiles of (a) surface temperature, (b) precipitation, (c) precipitable water, (d) soil moisture (averaged over the top three layers), (e) cloud fraction, and (f) planetary albedo.....	<b>28</b>
<b>Figure 3.3</b> Vertical profiles of cloud liquid water content ( $\text{g kg}^{-1}$ ) and cloud area fraction averaged over the low-latitude region ( $30^{\circ}\text{S}$ – $30^{\circ}\text{N}$ ) for the two terra-planet states in the simulations Z14 and Z15. ....	<b>29</b>
<b>Figure 3.4</b> Annual mean behaviour of <b>(a)</b> and <b>(b)</b> meridional stream function in $10^{10}\text{ kg s}^{-1}$ ; <b>(c)</b> vertical profiles of meridional transport of water at $10^{\circ}\text{N}$ for the two terra-planet states in the simulations.....	<b>31</b>
<b>Figure 3.5</b> Annual mean behaviour of northward transport of total, latent, and sensible energy in petawatts (PW) for the two terra-planet states in the simulations Z14 and Z15 averaged over a period of 10 years.....	<b>32</b>
<b>Figure 3.6</b> Annual mean surface temperature <b>(a)</b> , precipitation <b>(b)</b> , snow cover fraction <b>(c)</b> , and meridional stream function <b>(d)</b> for different stages of the transition (TRANS) simulation) .....	<b>34</b>
<b>Figure 3.7</b> Global mean surface temperature as a function of background soil albedo ( $\alpha$ ). Simulated HD states .....	<b>35</b>
<b>Figure 3.8</b> Annual mean meridional profiles as in Fig. 2 but with dark snow (snow albedo is the same as background soil albedo – DS simulations).....	<b>36</b>

<b>Figure 4.1</b> Hysteresis diagram showing the response of the surface temperature to changes in soil surface albedo from chapter 3. At low soil surface albedo ( $\alpha$ ) (high solar irradiation).....	<b>42</b>
<b>Figure 4.2</b> (a, b) Annual mean meridional profiles of surface temperature and precipitation, (c, d) vertical profiles of cloud area fraction averaged over the low latitude region (30°S - 30°N).....	<b>44</b>
<b>Figure 4.3</b> Low latitude feedback stabilizing the HD state for small perturbation and destabilizing the HD state .....	<b>47</b>
<b>Figure 4.4</b> Time evolution during the transition from the HD to the CW state at the bifurcation (simulation TRANS in Table 2.1).....	<b>49</b>
<b>Figure 4.5</b> Time evolution of surface precipitation (mm day <sup>-1</sup> ) in the low-latitude region during the transition from HD state to CW state (simulation “TRANS” in Table 2.1). The transition to the CW state.....	<b>50</b>
<b>Figure 4.6</b> Time evolution of (a) cloud cover and planetary albedo, (b) snow cover (%) (c) Precipitation (mm day <sup>-1</sup> ).....	<b>54</b>
<b>Figure. 5.1</b> shows the surface temperature response for different terra-planet simulations to varying soil surface albedo values for seven different obliquities ( $\theta$ ) varying from 0° to 23.5° .....	<b>55</b>
<b>Figure 5.2</b> Annual mean meridional profiles of (a) surface temperature, (b) precipitation, (c) snow cover, (d) precipitable water, (e) cloud fraction, and (f) evaporation for the three terra-planet.....	<b>58</b>
<b>Figure 5.3.</b> Annual mean behaviour of northward transport of total energy in petawatts (PW) for the three terra-planet states.....	<b>59</b>

# Abbreviations

**ICON** - ICOSahedral Non-hydrostatic

**LAI** - Leaf Area Index

**ITCZ** - Inter-Tropical Convergence Zone

**$\alpha$**  - Soil surface albedo

**$\emptyset$**  - Obliquity

**VPD** - Vapour Pressure Deficit



# Introduction

*Imagination will often carry us to worlds that never were. But without it we go nowhere. - Carl Sagan*

## 1.1 Background

In this dissertation, I examine how water recycling shapes the climate and circulation patterns of a homogenous land planet.

The Earth system is a complex combination of many subsystems – land, ocean and atmosphere – interacting with each other at various temporal and spatial scales. Our understanding of the Earth system is therefore based on the understanding of its various subsystems and interactions between them (Suni et al., 2015). ***This dissertation focuses on land-atmosphere interactions and their influence on the global climate.***

The land surface is the lower boundary for a large part of the atmosphere (about 29%). It strongly influences the climate on Earth by exchange of mass (water and carbon), radiation, heat, and momentum with the atmosphere (Suni et al., 2015). Land surface properties like albedo, roughness, soil moisture etc. govern the net energy balance at the surface through the partitioning of sensible and latent heat fluxes and have a huge effect on boundary layer dynamics and large scale circulation patterns on Earth. Climate in turn has an effect on the land surface – changes in climate can lead to changes in soil moisture and vegetation distribution.

Land-atmosphere interactions have been extensively studied for more than two decades using both observations and models of different complexities. While the effects of land surface on regional climates is well established, its effects on global climate are comparatively less understood. One of the reasons for this is the effects of land surface processes on global climate are often masked due to the overwhelming influence of oceans. A solution to this problem is to use simplified frameworks that can isolate the effects of land surface processes. Simple models and models of intermediate complexity were used in the past to understand the land-atmosphere interactions and feedbacks

(Brovkin et al., 1998; Zeng, 1999; Baudena et al., 2006, 2008; Aleina et al., 2013; Rochetin et al., 2014; Becker, T., and B. Stevens, 2014). However, most of these studies were based on one-dimensional (1-D) atmospheric models – single column atmospheric models, cloud-resolving models and radiative-convective models coupled to a simple land hydrology scheme (bucket model of soil). And all these studies were mainly focused on regional and local climate. But, to understand the effects of land-atmospheric coupling on global climate, comprehensive 3-D general circulation models are more useful. My study is an attempt in this direction. I consider a homogenous planet with no oceans and a globally extending continent with water mainly present in the soil and atmosphere. Such planets with vast deserts or vegetated surfaces and a limited amount of water (Herbert, 1965; Abe et al., 2005, 2011; Leconte et al., 2013; Aleina et al., 2013) are referred to as ‘terra-planets’. Such a terra-planet study with a 3-D general circulation atmospheric model could uncover mechanisms that are connected with land-atmosphere interactions and are not present on today’s Earth, but could be relevant in a different climate situation like in warmer climates or super continent configurations. Terra-planets are not completely unrealistic – Titan, the moon of Saturn, serves as the closest analogue for a dry terra-planet in our Solar System with a methane cycle instead of a water cycle. Most of its surface is dry with methane lakes at the poles. ***In this dissertation, I use a terra-planet setup for Earth-like conditions to investigate the effect of land-atmosphere coupling on global scale.***

## 1.2 Past studies on terra-planets

Most 3-D modelling studies on terra-planets are either about other terrestrial planets or Moons in our Solar System – Mars (Abe et al. 2005, 2011) and Titan (Mitchell et al., 2008, 2009) or about Habitable Exoplanets – planets that are suitable for supporting surface liquid water outside our Solar System (Zsom et al., 2013; Leconte et al., 2013).

Terra-planets can be the most promising candidates in the search for habitable planets due to the following reasons. Firstly, terra-planets with optically thin atmospheres (like present-day Earth’s atmosphere) can maintain their inner edge of the habitable zone<sup>1</sup> much closer to their parent star compared to aqua-planets (Zsom et al., 2013). This is because limited atmospheric access to water on such planets results in a

---

<sup>1</sup> habitable zone – range of orbits around a star within which a planet can support liquid water on its surface under certain pressure conditions (Kasting et al., 1993; Kopparapu et al., 2014)

dry climate with water confined to the high latitudes for low obliquities (Abe et al., 2005; Abe et al., 2011; Leconte et al., 2013). In such dry climates, the water vapour feedback is severely restricted and the greenhouse warming is substantially lowered, which allows dry planets to maintain habitability (stable surface liquid water) even at higher stellar fluxes (Zsom et al., 2013). Secondly, terra-planets at low obliquities can support a wider habitable zone compared to that of aqua-planets (Abe et al., 2011) because the dry atmosphere of terra-planets limits the escape of hydrogen molecules and shows a higher resistance to the runaway greenhouse effect. Also, the dry atmosphere inhibits the formation of clouds, ice, and snow and thus helps the planet to resist complete freezing (Abe et al., 2011; Leconte et al., 2013).

However, the habitable areas on such a dry planet are confined to the edges and bottom of frozen ice caps (Leconte et al., 2013; Zsom et al., 2013). Whether at such edges liquid water can exist sufficiently permanently for life to evolve and persist is unclear (Zsom et al., 2013). Recycling mechanisms similar to those which occur on the present-day Earth like ocean circulation and surface run-off must exist to maintain a long-lasting liquid water inventory. Leconte et al. (2013) argue that on dry planets, mechanisms like gravity-driven ice flows and geothermal flux can maintain sufficient amounts of liquid water at the edges and bottom of large ice caps. The liquid water thus formed can eventually flow back to the low latitudes to be re-available for evaporation. However, there is no climate modelling study on an Earth-like terra-planet which actually implements either implicitly or explicitly such a recycling mechanism bringing fresh water back from high to low latitudes.

***In this thesis, I try to fill this gap by considering an Earth-like terra-planet with an unlimited subsurface water reservoir as a way to mimic the recycling mechanism to investigate the effect of water recycling on the climate of low-obliquity Earth-like terra-planets.***

It should be noted that, although the water reservoir in my case is unlimited, it is not similar to an aqua-planet because it includes additional resistances which restrict atmospheric access to water (i.e. soil and plant resistances along with aerodynamic resistance).

### 1.3 Multiple climate states

Feedbacks within a system can result in multiple stable states for the same environmental conditions. Such systems with multiple equilibria can show increased sensitivity to natural variability or external perturbations (Scheffer et al., 2001). And strong perturbations can push the system from one stable state to the other. Previous studies on land-atmosphere coupling with simple 1-D models confirm the existence of multiple equilibria in the land-atmosphere system. For example, bimodality in soil moisture and precipitation was reported for regional climate in a simple land-atmosphere model (Rodriguez-Iturbe et al. 1991 a,b; Entekhabi et al. 1992, 1995), Brubaker and Entekhabi 1995 found bi-modality in surface Bowen ratio due to land and boundary layer interactions. More recently, Aleina et al., 2013 demonstrated multiple equilibria due to climate-vegetation interactions using a conceptual 1-D terra-planet setup. Rochetin et al., 2014 also found multiple equilibria in a Radiative Convective model coupled to a land surface. Contrary to these 1-D model studies, 3-D modelling studies of Earth-like terra-planets for low-obliquities ( $< 30^\circ$ ) report only one stable climate state – a hot climate state with all water trapped permanently in ice caps at high latitudes (Abe et al., 2005, 2011).

### 1.4 The effect of obliquity on the climate of terra-planets

Obliquity or axial tilt – the angle between the rotational axis and the orbital axis of an astronomical object – varies widely among planets. In our Solar System Mercury has an obliquity of  $0^\circ$ , Venus  $2.6^\circ$ , Earth  $23.5^\circ$ , and Uranus  $82.1^\circ$ . Obliquity is the reason for a seasonal cycle of solar insolation and thereby controls the latitudinal distribution of solar energy received by a planet: the higher the obliquity the more evenly distributed the annual average solar insolation between the poles and the equator. Therefore, obliquity is one of the key governing factors of climate on any planet (Kilic et al., 2017). Changes in obliquity modify the latitudinal distribution of surface temperature on a planet, the strength of the atmospheric and oceanic energy transport from warmer to colder regions, the snow cover distribution, and the spatial pattern as well as the intensity of precipitation. As a consequence, several climate states and transitions between them could emerge with changes of obliquity.

Recent studies on water dominated planets have confirmed the existence of multiple climate states and potential transitions between different climate states for a

range of obliquity values and solar irradiation (Kilic et al., 2017; Linsenmeier et al., 2015). These studies demonstrated that seasonal variability can strongly influence the existence of different climate states and transitions between them (Linsenmeier et al., 2015). Conversely, for water-limited planets (terra-planets), the effect of obliquity on climate is not well understood. Past studies report that for a range of obliquity values less than 30°, terra-planets can only exhibit one climate state – a hot climate state with all water trapped permanently in ice caps at high latitudes as discussed in Sect 1.3 (Abe et al., 2005; 2011).

***Hence, in this dissertation using a 3-D general circulation model equipped with an overland water recycling<sup>2</sup> mechanism I investigate the possibility of multiple climate states for Earth-like terra-planets over a range of soil surface albedo values and obliquity.***

## 1.5 Thesis Outline

The main aim of this thesis is to investigate the role of water recycling in shaping the climate of Earth-like terra-planets. I do this by answering the following research questions.

- What is the effect of water recycling on the climate of Earth-like terra-planets? (**chapters 3,4,5**)
- Can Earth-like terra-planets equipped with a water recycling mechanism exhibit multiple climate states for the same boundary conditions? Can abrupt transitions occur between different climate states? (**chapters 3,4,5**)
- Which processes are responsible for the stability of different climate states? What mechanisms lead to abrupt transitions between the climate states? (**chapter 4**)
- How does seasonal variability affect multistability and bifurcations on Earth-like terra-planets? (**chapter 5**)

For answering each of the questions listed above, a series of idealised simulations are performed with the 3-D General Circulation Model ICON with dynamic land hydrology in terra-planet configuration including a water recycling mechanism. The details of the

---

<sup>2</sup> The fresh water recycled from high to low latitudes through rivers and underground flows is referred to in this thesis as the “overland water recycling mechanism”

model, terra-planet setup, water recycling mechanism and different simulations performed for this study are discussed in *chapter 2*.

In *chapter 3*, I investigate the climate of Earth-like terra-planets with a water recycling mechanism for perpetual equinox (zero obliquity) conditions. I also explore the possibility of multiple climate states and transitions between different climate states by varying the soil surface albedo values. This work has been published in the Journal of Earth system Dynamics<sup>3</sup> and text is modified to fit the format of this thesis.

*Chapter 4* examines the mechanisms responsible for the existence of multiple climate states and bifurcations on Earth-like terra-planets. *Chapter 5* explores the sensitivity of multistability discussed in *chapter 3* to seasonal variability. This is done by repeating the analysis in *chapter 3* for non-zero obliquities. I then compare the findings for perpetual equinox conditions (*chapter 3*) and non-zero obliquities (*chapter 5*). In *chapter 6*, I summarise the main findings from different chapters and propose directions for future research.

---

<sup>3</sup> Kalidindi, S., Reick, C. H., Raddatz, T., and Claussen, M. (2018): Two drastically different climate states on an Earth-like terra-planet, Earth Syst. Dynam., 9, 739-756, <https://doi.org/10.5194/esd-9-739-2018>.

# 2

## Model and simulation setup

### 2.1 Model

I use the ICOSahedral Non-hydrostatic (ICON) General Circulation Model jointly developed by the MPI for Meteorology and the German Weather Service (DWD) and run it in terra-planet configuration i.e. with a single globally extended continent. The model has a horizontal resolution of R2B04 equivalent to a resolution of an evenly distributed rectangular grid of about  $\sim 160$  Km and 47 layers in the vertical. The atmosphere model uses a non-hydrostatic dynamical core on an icosahedral-triangular Arakawa C-grid (Zangl et al., 2015), and the model atmospheric physics is similar to ECHAM6 physics (Stevens et al., 2013). The radiative transfer calculations are based on the Rapid Radiative Transfer Model (Mlawer et al., 1997; Iacono et al., 2008). Convection is parameterized by the mass flux scheme of Tiedtke (1989) with modifications to penetrative convection by Nordeng (1994). Cloud cover is calculated based on relative humidity (Lohmann and Roeckner, 1996). For a complete description of the model physics and parameterizations, the reader is referred to Stevens et al. (2013). The ICON version used in this study inherits the land physics from ECHAM5 (Roeckner et al., 2004) extended by a layered soil hydrology (Hagemann and Stacke, 2015).

### 2.2 Terra-planet configuration

The Terra-planet configuration is designed to be highly symmetric with no orography and glaciers. The rotation rate and the solar constant are the same as for the present day Earth. Background concentration of  $\text{CH}_4$ ,  $\text{N}_2\text{O}$  and aerosols are fixed to zero, while water vapor is prognostic and  $\text{CO}_2$  concentration in the atmosphere is fixed to 348 ppmv. The ozone distribution is assumed to be zonally uniform and meridionally symmetric.

Land surface properties are assumed to be homogenous: The total soil depth in my study is about 10 meters (m) of which the layers below a depth of 1.2 m are forced to be filled permanently by at least 90% with water homogeneously all over the globe. I refer

to these bottom two layers of the soil in my study as 'subsurface reservoir' which should not be confused with a geological reservoir operating at timescales much longer than the soil hydrological timescales. The root depth is fixed to 6 m such that the roots always have access to this subsurface reservoir. Leaf Area Index (LAI) is set to a value of 3. This value controls how much surface in a grid cell participates in transpiration, while the rest exhibits bare soil evaporation. LAI and root depth are not considered as a representation of vegetation but only as a technical means to parameterize the atmospheric access to water like other hydrological parameters of the model, e.g. soil porosity or hydraulic conductivity. The albedo of snow ranges between 0.4 - 0.8 depending on the surface temperature. Surface roughness is fixed to 0.05 m.

By the introduction of the subsurface reservoir I implicitly equip my planet with a very efficient recycling mechanism shuffling water back from sink regions ( $P-E > 0$ ) to source regions ( $P-E < 0$ ). This can be understood as follows. In sink regions water either piles up as snow or is lost as runoff. But since neither snow height nor runoff affect the climate in my simulations, the global amount of water relevant for the physical climate stays constant for a stationary state. Accordingly, considering only this 'effective' water, the amount of water added to the subsurface reservoir equals the water lost in the sink regions. For this reason, I can interpret the permanent refilling of the subsurface reservoir to mimic a very efficient recycling of water from sink to source regions.

Representing overland water recycling by a homogeneously filled subsurface reservoir is indeed an idealization. In fact, recycling may occur at different speeds and thereby is less or more effective than what I consider in my study. Based on the speed of recycling, the water level of this subsurface reservoir would vary from what is considered in my study. It should be noted that the choice of water level of the subsurface reservoir considered in my study (1.2 m) is not arbitrary, but a result of a sequence of simulations, where I explored the continuum between an aqua and a terra planet (see Sect. 2.4).

My terra-planet setup closely resembles that of recent 3-dimensional studies (Abe et al., 2011; Leconte et al., 2013) on Earth-like terra-planets except that those studies did not consider an overland water recycling pathway bringing back water from high to low latitudes that I mimic by the prescribed subsurface water reservoir.

## 2.3 Simulations

I consider two situations: perpetual equinox (zero obliquity) and non-zero obliquity. For each of these situations, I study the effect of background surface albedo ( $\alpha$ ) on the climate in a series of simulations with  $\alpha$  varying from 0.07 to 0.24 at perpetual equinox ( $0^\circ$ ) (Z7 to Z24 simulations in Table 2.1) and at non-zero obliquity ( $3^\circ, 5^\circ, 10^\circ, 15^\circ, 23.5^\circ$ ) (S2 to S17 simulations in Table 2.1). All these simulations start from the same initial atmospheric state with a homogenous temperature (290 K) and moisture content ( $25 \text{ kg m}^{-2}$ ). Due to the small thermal inertia of the land surface and the atmosphere, the simulations reach a steady state within 10 years. The simulations are continued for additional 30 years of which, the last 10 years are used in the analysis of the mean climate. To understand the transition between different terra-planet climate states at the perpetual equinox condition more clearly, I perform an additional simulation (TRANS). For this, I first simulate the planet in the stable Hot and Dry (HD) state for 30 years for  $\alpha = 0.14$  and then increase  $\alpha$  abruptly to  $\alpha = 0.14 + 0.01$  corresponding to the Cold and Wet (CW) state and continue the simulation for another 30 years. Then, to check for hysteresis, I continue the TRANS simulation by switching the albedo back to 0.14 and continue lowering  $\alpha$  stepwise until zero. To investigate the role of snow-albedo feedback on the terra-planet climate states, the terra-planet is simulated with dark snow at perpetual equinox conditions (DS simulations in Table 2.1) (i.e. I assume snow albedo to be same as background surface albedo). Additionally, to test the sensitivity of the climate states to model parameterizations, I performed simulations with a different convection scheme at perpetual equinox conditions (T7 to T24 simulations).

The effect of obliquity on the mean climate of a terra-planet (situation 2) is investigated with different sets of idealised terra-planet simulations where in the soil surface albedo  $\alpha$  is varied in the range of 0.02 – 0.17 (similar to the method followed for perpetual equinox situation) for seven different values of obliquities ( $3^\circ, 5^\circ, 10^\circ, 15^\circ, 23.5^\circ$ ). The analysis in this thesis is restricted to lower obliquities. This is because for higher obliquities, the seasonal variability gets very extreme which can lead to more complicated climate and circulation patterns which is beyond the scope of the present thesis. The eccentricity in all simulations is fixed to zero. All the simulations are started from an initial atmospheric state with a homogenous temperature of 290 K, moisture content of  $25 \text{ kgm}^{-2}$ . The simulations are run until a steady state is reached. To check for

bistability and hysteresis, for each value of obliquity, the soil surface albedo  $\alpha$  is increased from 0.02 – 0.17 and decreased again from 0.17 to 0.02 (S2 to S17 simulations in Table 2.1). This allows to check how the bistability observed in for zero obliquity (existence of both HD and CW state for the same soil surface albedo values) is affected by obliquity. It should be noted that threshold of bistability is different for different obliquity values, hence the soil surface albedo is varied (increased or decreased) accordingly based on the particular threshold value. The details of all terra-planet simulations are listed in Table 2.1.

Simulations	Background soil albedo	Obliquity	Convection scheme	Snow albedo
<b>Z7 – Z24</b>	0.02, 0.07, 0.12, 0.14, 0.15, 0.17, 0.24	0	Nordeng	Dynamic
<b>S2 – S17</b>	0.02 - 0.04 - 0.07 - 0.12 - 0.14 - 0.15 - 0.17 and reverse: 0.15 – 0.14 – 0.07 – 0.04- 0.02	3, 5, 10, 15, 23	Nordeng	Dynamic
<b>TRANS</b>	0.14 – 0.15 – 0.14 – 0.12 – 0.07- 0.00	0	Nordeng	Dynamic
<b>T7 – T24</b>	0.07, 0.12, 0.14, 0.15, 0.17, 0.24	0	Tiedtke	Dynamic
<b>DS</b>	0.07, 0.12, 0.14, 0.15, 0.17, 0.24	0	Nordeng	Constant at background soil albedo

*Table 2.1. Summary of simulations performed in this study.*

## 2.4 Sequence of simulations that led to the discovery of the terra-planet bi-stability

The bistability was found by systematically modifying the ICON-ESM global climate model starting from a “swamp simulation” until a “terra-planet configuration”. The respective simulations showed climate states that were plausible from the configuration changes. In the swamp configuration the model is able to successfully reproduce the climate of an aqua-planet. Starting from this set-up, I sequentially changed different parameters like surface heat capacity, surface roughness, background soil albedo, snow albedo, and the level of the global subsurface water reservoir as well as the land surface schemes (soil hydrology) in the land surface model (Table 2.2). The bistability emerged when the water level of the subsurface reservoir was lowered to 1.2 m. In Table 2.2 the sequence of

simulations is listed and in Fig. 2.1 I show the resulting time evolution of temperature and the zonal structure of precipitation. Therefore, the bistability is not a result of a random experiment or a bug in the land surface model.

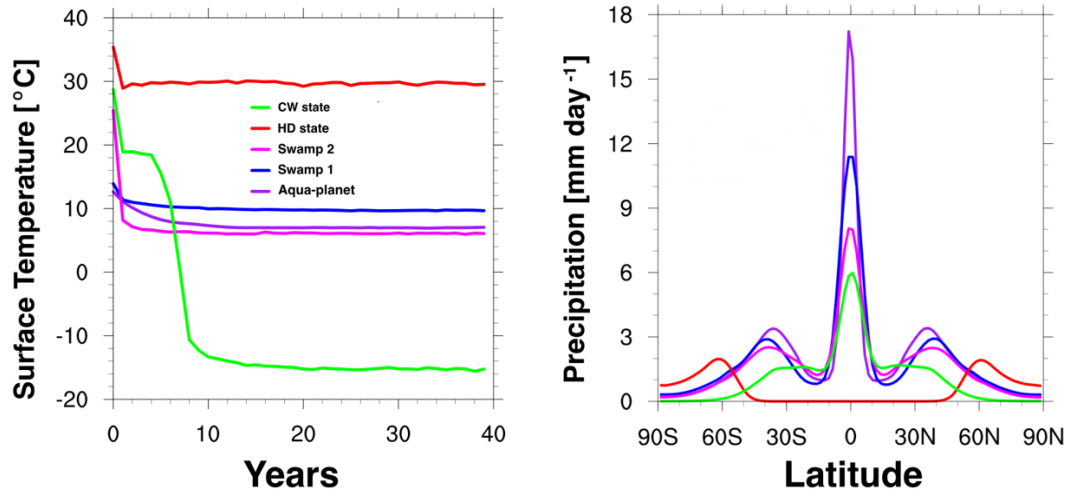


Figure 2.1 (a) Time series of global mean surface temperature (°C) and (b) annual mean meridional profile of precipitation (mm day<sup>-1</sup>) for different simulations performed to illustrate the procedure by which I found bistability on my terra-planet.

Simulations	Background soil albedo	Surface roughness	Heat capacity	Snow albedo	Water reservoir depth
Aqua-planet	0.07	Ocean	Ocean	0.07	50 m slab ocean, no heat transport
Swamp1	0.07	Ocean	Ocean	0.07	Constant ground water table at a depth of 0.3 m
Swamp2	0.07	Land	Land	0.07	Constant ground water table at a depth of 0.3 m
HD	0.07-0.14	Land	Land	Dynamic (0.4 -0.8)	Constant ground water table at a depth of 1.2 m
CW	0.15-0.24	Land	Land	Dynamic (0.4 -0.8)	Constant ground water table at a depth of 1.2 m

Table 2.2 Summary of simulations performed to illustrate the procedure followed by which I found bistability on my terra-planet.



# 3

## Drastically different climate states for perpetual equinox

### 3.1 Mean climate

Figure 3.1 shows the time evolution of global mean surface temperature and precipitation for different terra-planet simulations at zero obliquity (Z7 to Z24 simulations). I notice that the terra-planet exists in two drastically different climate states: HD state for  $\alpha < 0.15$  and a CW state for  $\alpha \geq 0.15$ . This is different from findings in previous studies (Abe et al., 2005, 2011; Leconte et al., 2013) on low-obliquity terra-planets in which only the HD state was found. The mean climate in the two states is remarkably different (Fig. 3.2).

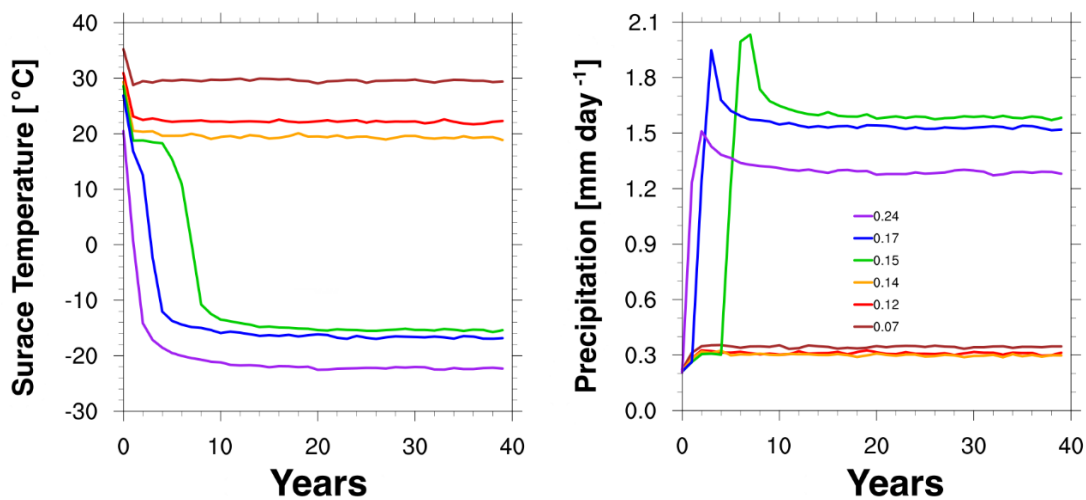


*Figure 3.1* Time series of global mean surface temperature ( $^{\circ}\text{C}$ ) and precipitation ( $\text{mm day}^{-1}$ ) for different soil surface albedo values in the Z7–Z24 simulations in Table 2.1.

#### 3.1.1 Surface temperature

The annual mean surface temperature in the CW state is below freezing point almost everywhere, except in the low latitudes where it is around  $10^{\circ}\text{C}$ . High cloud cover (Fig. 3.2e) and a high planetary albedo (Fig. 3.2f) lower the surface absorption of incoming radiation and result in very low temperatures in the CW state. However, in the HD state, the global mean surface temperature is about  $35^{\circ}\text{C}$  higher than in the CW state.

### 3.1.2 Precipitation

In addition to temperature, the other striking difference between the two states is the location of precipitation bands on the planet. In the HD state, no precipitation occurs in the low-latitude region between 40° S and 40° N. Only latitudes higher than 40° receive some amount of rainfall (Fig. 3.2b) (compare Abe et al., 2005, 2011; Leconte et al., 2013). In contrast, in the CW state, precipitation is mainly concentrated in the low latitudes with a banded structure similar to the present-day equatorial Inter-Tropical Convergence Zone (ITCZ). The reason for the absence of a CW state in previous studies is the lack of an effective mechanism that can recycle the water trapped at the high latitudes in the form of snow and ice back to the low latitudes.

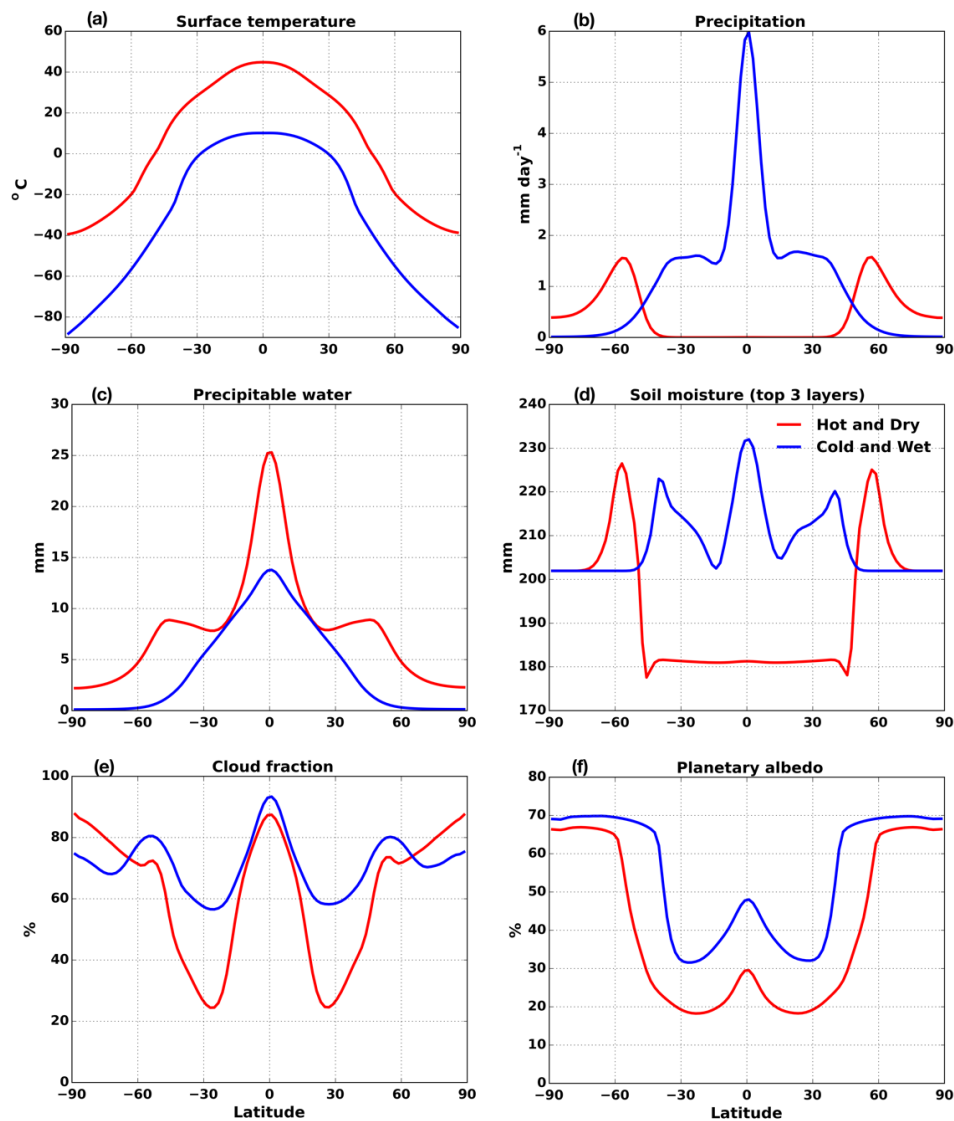


**Figure 3.2** Annual mean meridional profiles of (a) surface temperature, (b) precipitation, (c) precipitable water, (d) soil moisture (averaged over the top three layers), (e) cloud fraction, and (f) planetary albedo for the two terra-planet states: HD ( $\alpha = 0.14$ ) and CW ( $\alpha = 0.15$ ) in the simulations Z14 and Z15 averaged over a period of 10 years.

### 3.1.3 Feedbacks that keep the HD state dry and the CW state wet

Figure 3.2c and d show the distribution of water on the planet. In the HD state, the very high temperatures in the low latitudes raise the water vapour saturation limit and the moisture-holding capacity of the atmosphere, allowing the planet to store a substantial amount of its water in the atmosphere (Fig. 3.2c). In such an atmosphere, rain occurs in the form of virga rain, i.e. almost all of this rain evaporates on its way to the surface. Therefore, in such a case, rain does not contribute to the moistening of the soils in the low latitudes. This, along with huge amounts of net radiation at the surface in the HD state, keeps the uppermost soil layers in the low latitudes very dry. Dry uppermost soil layers imply small evaporation, leading to no precipitation, which in turn leads to even less evaporation. This self-reinforcing mechanism in the HD state always maintains very dry upper soil layers in the low latitudes (Fig. 3.2d). On the whole, suppressed precipitation at low latitudes along with a nevertheless permanent export of moisture away from the low latitudes result in water being mainly present at high latitudes in the HD state. Conversely, in the CW state, the lower annual mean temperatures in the low latitudes facilitate condensation and precipitation and minimize the moisture content of the atmosphere (Fig. 3.2c). Evaporation of falling rain indeed also occurs in the CW state but is not strong enough to prevent the rain from reaching the surface. Thus, continuous precipitation at low latitudes in the CW state keeps the upper soil layers in the low latitudes always wet (Fig. 3.2d) thus providing sufficient water by evaporation for a stable precipitation regime in the low latitudes.

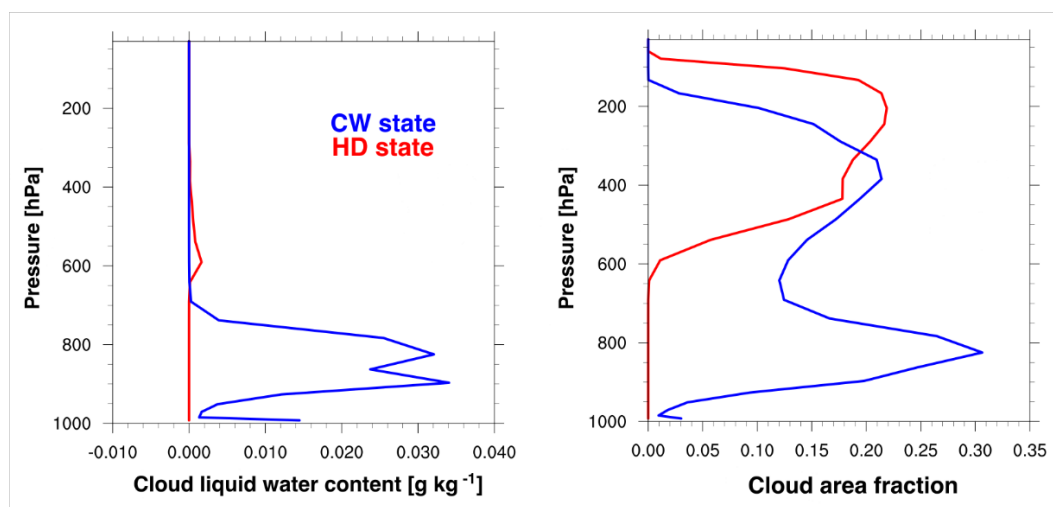


**Figure 3.3** Vertical profiles of cloud liquid water content ( $\text{g kg}^{-1}$ ) and cloud area fraction averaged over the low-latitude region ( $30^\circ \text{S}$ – $30^\circ \text{N}$ ) for the two terra-planet states in the simulations Z14 and Z15.

### 3.1.4 Feedbacks that keep the HD state hot and CW state cold

The vertical distribution of cloud cover and cloud water content in the low latitudes for the two terra-planet states is displayed in Fig. 3.3. For the HD state, the cloud cover in the low latitudes is exclusively composed of high level clouds (Fig. 3.3). The reason is that the higher water vapour saturation limit of the atmosphere in the HD state raises the height at which condensation and cloud formation occur. High clouds with very low liquid water content are more transparent to shortwave radiation; at the same time, they reduce outgoing longwave radiation and thereby warm the planet. Moreover, hotter temperatures in the HD state lead to a moister atmosphere (Fig. 3.2c) and in turn stronger greenhouse warming. Overall, high clouds in the low latitudes along with higher water vapour greenhouse warming keep the planet always hot and stabilize the HD state. Instead, in the CW state, the cloud cover in the low latitudes is mainly comprised of low-level clouds (Fig. 3.3) due to a lower water vapour saturation limit of the atmosphere. Low clouds with high liquid water content cool the planet as they increase the planetary albedo. Also, lower temperatures in the CW state lead to a drier atmosphere (Fig. 3.2c) and a weaker water vapour greenhouse warming. On the whole, low clouds together with weaker greenhouse warming always keep the planet cool and stabilize the CW state.

### 3.1.5 Mean circulation and energy transport

The mean circulation pattern for the two climate states is shown in Fig. 3.4 a and b. In both the states, the circulation pattern resembles the present-day three-cell hemispheric structure. But when comparing the two states, the width and intensity of the circulation are very different: in the HD state, the Hadley cell is more vigorous and becomes slightly wider with height (when measured around 500 hPa) compared to that in the CW state. The neutrally stable atmospheric conditions found in the HD state require a larger mass flux to transport away heat and to stabilize the equatorial temperatures and hence support a more vigorous circulation (Held and Hou, 1980; Caballero et al., 2008; Mitchell, 2008). Additionally, I notice that the circulation centre of the Hadley cell is very different in the two states (depicted by black arrows in Fig. 3.4a and b). The HD state has its circulation centre much closer to the surface at about 750 hPa, while in the CW state the centre is much higher at 500 hPa.

Observations and modelling studies in the literature also report intense low-centred circulations for present-day Earth's climate in the tropical eastern pacific during the northern hemispheric summertime (Zhang et al., 2004, 2008; Nolan et al., 2007), for

a Snowball Earth state (Pierrehumbert, 2005) and for Titan (Mitchell et al., 2006, 2009). These circulations have the tendency to export larger amounts of moisture out of the low latitudes compared to high-centred circulations. I also notice this increased transport of moisture away from the low latitudes with the more vigorous low-centred Hadley cell in the HD state compared to that in the CW state (Fig. 3.4c). The reason is that in the CW state the existence of deep convection allows moisture to reach much higher elevations before being exported to high latitudes (Nolan et al., 2007). At higher elevations, more moisture can condense and be lost as precipitation due to low temperatures and thus much less water remains for being exported away. Instead, in the HD state the lack of precipitation allows more moisture to be exported.

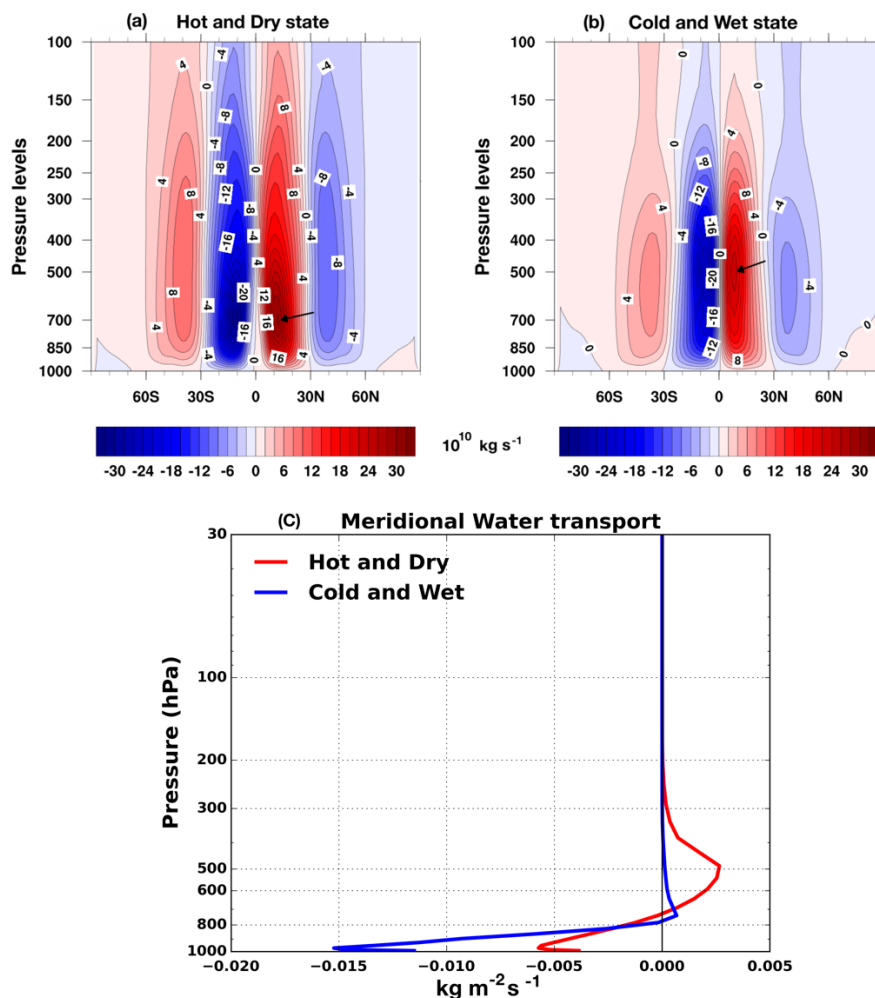


**Figure 3.4** Annual mean behaviour of (a) and (b) meridional stream function in  $10^{10} \text{ kg s}^{-1}$ ; (c) vertical profiles of meridional transport of water at  $10^\circ \text{ N}$  for the two terra-planet states in the simulations Z14 and Z15 averaged over a period of 10 years. The black arrows in (a) and (b) denote the northern Hadley circulation centre.

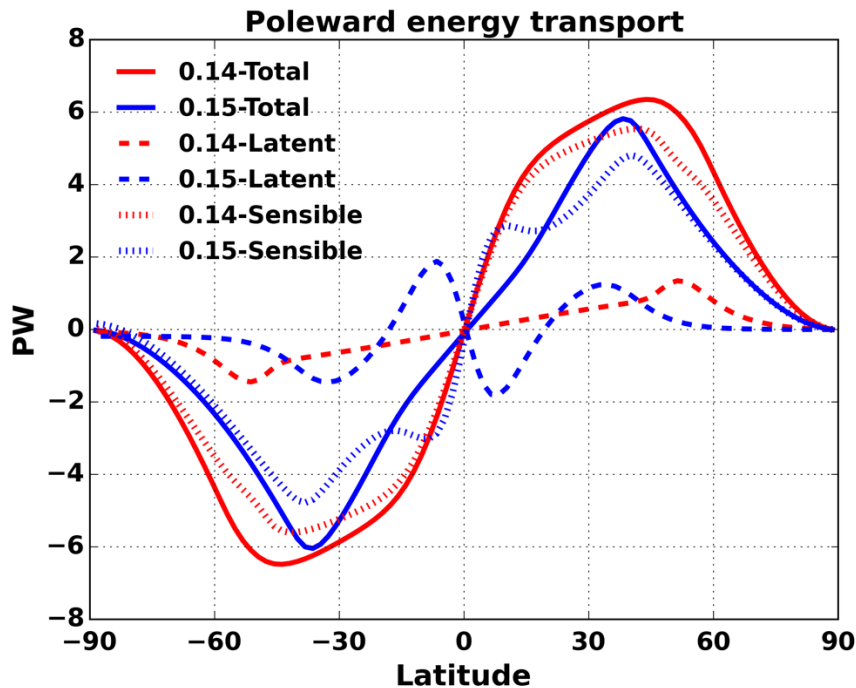


*Figure 3.5* Annual mean behaviour of northward transport of total, latent, and sensible energy in petawatts (PW) for the two terra-planet states in the simulations Z14 and Z15 averaged over a period of 10 years.

Figure 3.5 shows the northward transport of energy (transport due to latent and sensible energy) by atmospheric circulation in the two climate states. For the CW state, latent energy transport is equatorward in the low latitudes and poleward in the mid-latitudes. In contrast, in the HD state latent energy is exported poleward at all latitudes (latent energy curves in Fig. 3.5). The reason for the opposite sign in the low latitudes is that in the CW state (as in the case of present-day Earth) intense precipitation dries out the atmosphere and thus keeps most of the water within the low latitudes, limiting its poleward export (Fig. 3.4c) – hence at these latitudes the net flow is always equatorward. Instead, in the HD state, by the absence of precipitation, moisture is retained in the air so that it is exported poleward.

The sensible energy transport in the HD state is considerably larger as compared to that in the CW state (Fig. 3.5) despite a lower equator-to-pole temperature gradient. This implies that the atmospheric circulation is more efficient in transporting the sensible energy to the high latitudes. Nevertheless, the net northward transport of energy is dominated by the sensible energy transport. Further, the larger northward transport of

energy in the HD state results in a smaller equator-to-pole temperature gradient compared to the CW state.

### 3.2 Transition to the CW state

Starting from the HD state ( $\alpha = 0.14$ ), I abruptly increase the albedo to  $\alpha = 0.14 + 0.01$  (simulation TRANS in Table 2.1) and thereby initiate a shift to the CW state. The full transition from the HD state to the CW state takes about 4 years. The changes in annual mean surface temperature, precipitation, snow cover, and mean circulation during the course of transition are shown in Fig. 3.6. One can distinguish three transitional stages.

- **Stage 1.** After the abrupt increase in  $\alpha$ , small precipitation clusters appear in the low-latitude region and the terra-planet starts to cool down due to an increase in cloud cover and planetary albedo. Snow cover at high latitudes starts to increase slowly. The mean meridional circulation structure changes – small circulation cells appear very close to the equator. This happens for a period of 1 year.
- **Stage 2.** The precipitation clusters aggregate into a band of deep convection around the equator accompanied by a sharp increase in precipitation. At this point, I still see precipitation bands even at high latitudes around  $50^\circ$ . However, the precipitation intensity at high latitudes is smaller (around  $6 \text{ mm day}^{-1}$  lower) compared to the precipitation at the equator. Surface temperature drastically decreases and the circulation structure is now associated with two cells, a shallow cell close to the equator and a deep cell slightly away from the equator.
- **Stage 3.** Precipitation bands at the high latitudes start moving equatorward and precipitation intensity decreases compared to the previous stage. Surface temperature decreases further. Snow cover further increases and starts moving towards the equator. The circulation is now less intense with a circulation centre around 500 hpa.

Finally, the CW state is reached. Precipitation only occurs at low latitudes. Surface temperature is below freezing almost everywhere on the planet except at the low latitudes. Snow cover reaches down to  $40^\circ$  latitude.

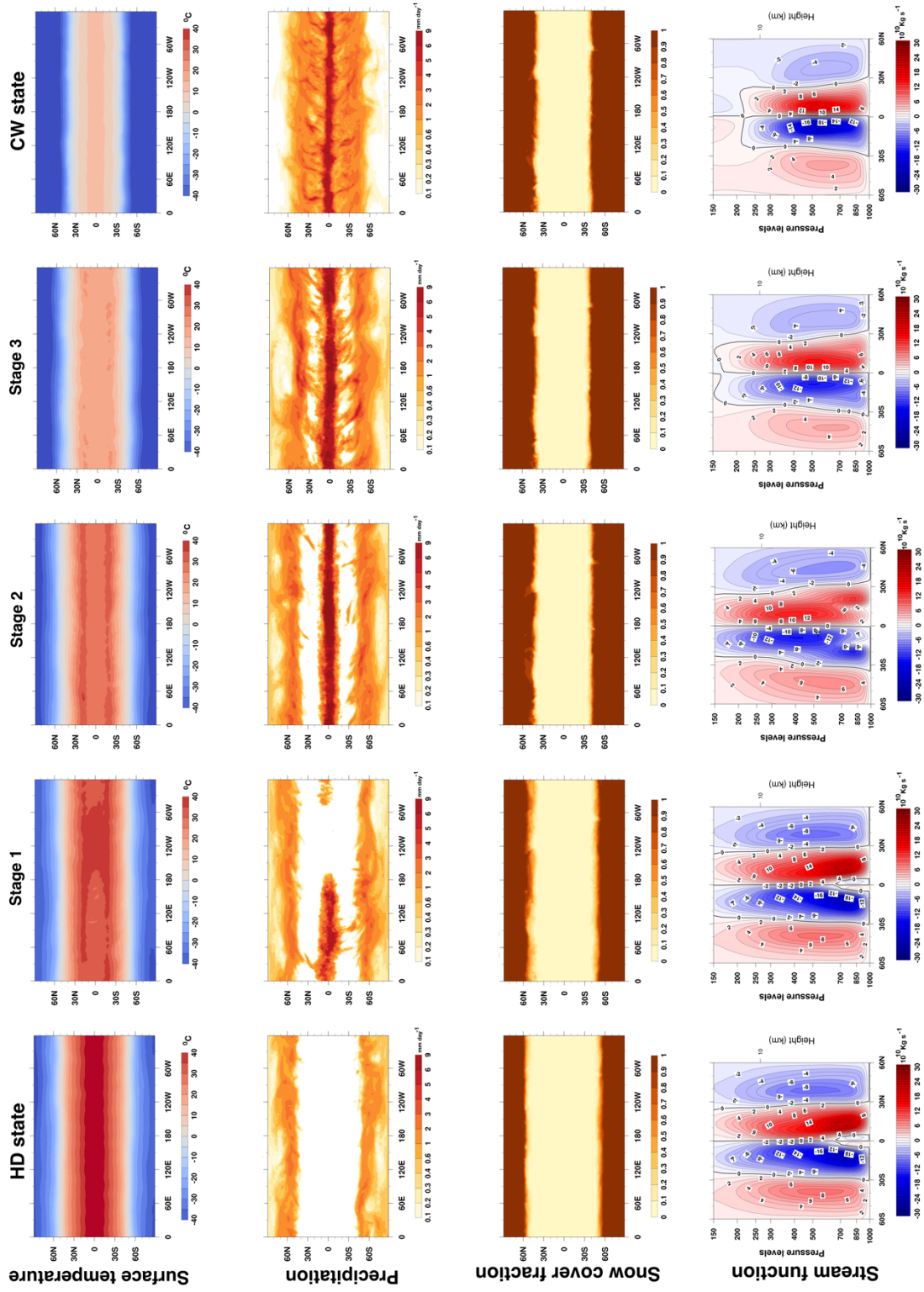
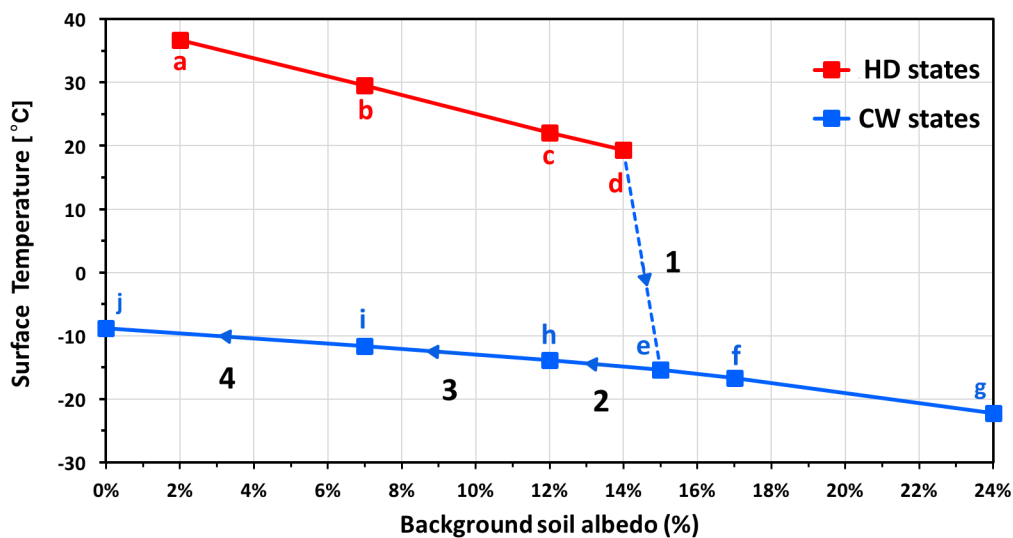


Figure 3.6 Annual mean surface temperature (a), precipitation (b), snow cover fraction (c), and meridional stream function (d) for different stages of the transition (TRANS) simulation) from the HD state to the CW state.

### 3.3 Hysteresis

To further study the bifurcation structure, I investigated the hysteretic behaviour. Figure 3.7 shows the global mean surface temperature plotted as a function of  $\alpha$ . The spontaneous transition from the HD to the CW state and the associated abrupt cooling is seen as path 1. Starting from the CW state and lowering back  $\alpha$  stepwise below the threshold value until zero does not lead back to the HD state. The reason is that the high cloud cover present in the CW state hides the surface from solar irradiation. Therefore, a reduction of  $\alpha$  has only a minor effect on the top-of-the-atmosphere radiation balance so that thereby it is impossible to heat the planet sufficiently strongly to switch back to the HD state. This is true even when repeating these simulations with snow albedo equal to background soil albedo (DS experiments; no figure shown). Thus, the planet remains in the CW state, indicating that under the chosen conditions for the terra-planet set-up the hysteresis is not closed (Fig. 3.7).



**Figure 3.7** Global mean surface temperature as a function of background soil albedo ( $\alpha$ ). Simulated HD states are denoted by points a–d and simulated CW states by e–j. Path 1 denotes the spontaneous transition from HD to CW when increasing  $\alpha$ , and paths 2–4 denote the reverse state development upon stepwise lowering of background albedo starting from the threshold value until zero. Obviously, the hysteresis does not close for the terra-planet at zero obliquity considered here.

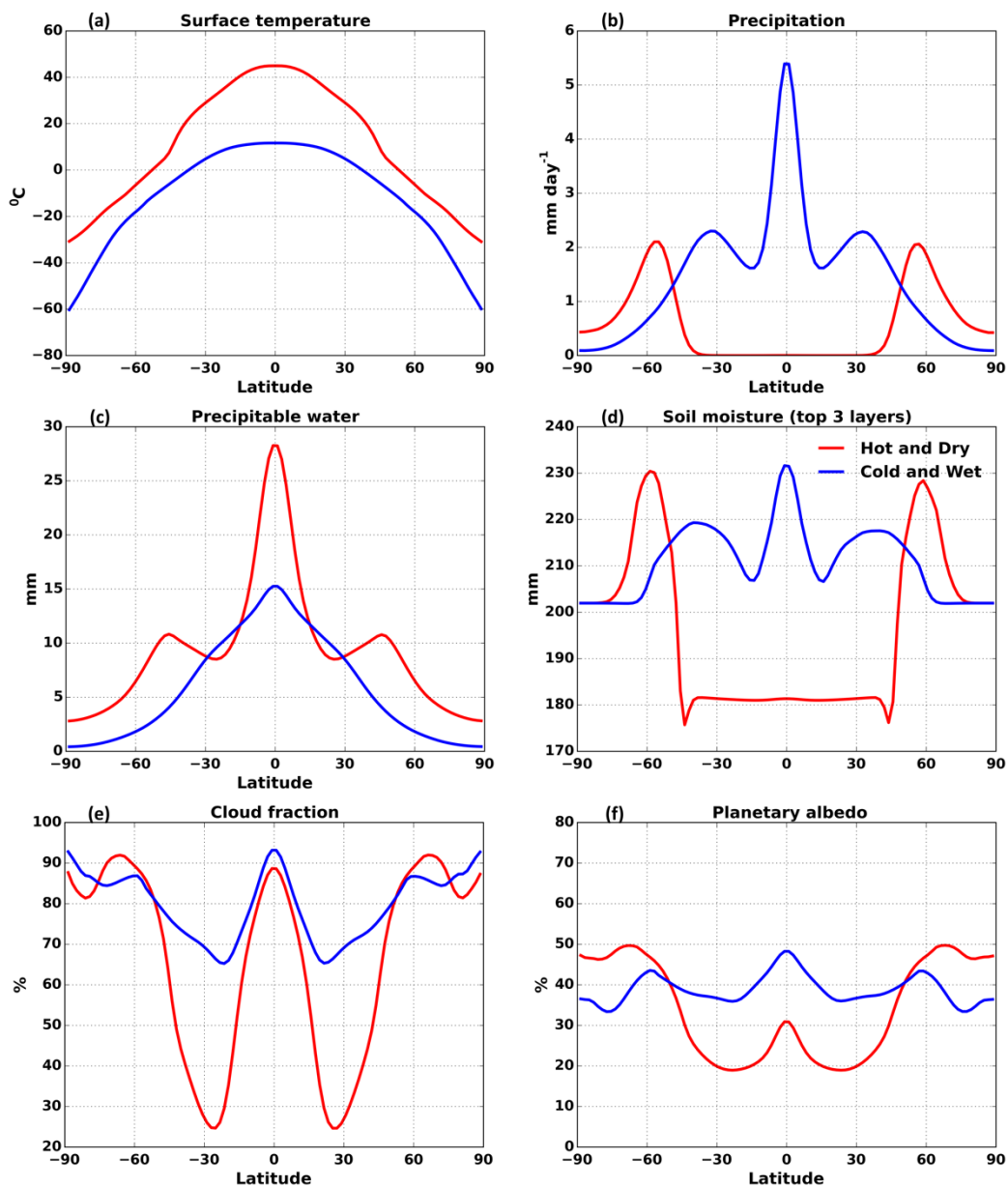


*Figure 3.8 Annual mean meridional profiles as in Fig. 3.2 but with dark snow (snow albedo is the same as background soil albedo – DS simulations).*

### 3.4 Does snow albedo feedback play a role in the emergence of the two climate states?

Changes in snow cover can lead to multiple climate states in the Earth system with drastically different global mean surface temperatures like present-day Earth and Snowball Earth (Budyko, 1969; Sellers, 1969). In this case, the large temperature

difference between the two states is caused by the positive snow albedo feedback. In my study, I also notice such a huge difference in global mean surface temperature between the two terra-planet climate states (Sect. 3.3). In order to test whether the snow albedo feedback is responsible for the huge temperature difference in my study, I performed additional simulations in which I changed the snow albedo to be equal to the background albedo of soil (DS simulations in Table 2.1). With the darker snow, I still find the two climate states (Fig. 3.8) and the spontaneous transition between them. The existence of the bifurcation even in the simulations with dark snow implies that the snow albedo feedback is not the cause of the existence of the two states. However, the snow albedo feedback does enhance the drastic temperature change in the bright snow simulations by around 12 °C compared to the dark snow simulations.

### 3.5 Discussion and conclusions

So far terra-planets have been investigated for a wide range of planetary properties like mass, rotation rate, atmospheric composition, and orbit (Abe et al., 2005, 2011; Leconte et al., 2013). Here, I focus on climate simulations of a terra-planet with zero obliquity, flat orography, and otherwise Earth-like conditions. An important difference from previous studies concerns the treatment of atmospheric access to water. Past studies on possible climates of terra-planets prescribed a limited water inventory, which for low obliquities leads to trapping of the water at high latitudes, stabilizing the planet in a state with no precipitation at low latitudes, similar to what I call the hot and dry state in my study. By contrast, in the present study I assume an unlimited subsurface water reservoir, which is still different from an aqua-planet configuration (also with an unlimited water reservoir), because resistances between soil and atmosphere restrict the atmospheric access to soil water in addition to the restriction from aerodynamic resistance. For such an Earth-like terra-planet with restricted water access I find two drastically different climate states, a HD state characterized by a hot climate with precipitation confined to high latitudes and a CW state which is closer to present-day Earth's climate with precipitation mainly occurring at low latitudes and an intense cycling of water there. Compared to the other studies mentioned above, I only find this additional CW state because by prescribing the subsurface water reservoir I implicitly assume a mechanism restoring water from the high latitudes to low latitudes for my terra-planet, refilling the subsurface water reservoir sufficiently effectively to maintain the very active low-latitude water cycle in this state.

The difference in global mean temperature between these two climate states is 35 °C (with the same boundary conditions), which is of the same order of magnitude as the temperature difference between present-day and Snowball Earth climate (Pierrehumbert et al., 2011; Micheels and Montenari, 2008; Fairchild and Kennedy, 2007; Hoffman and Schrag, 2002).

Similar to the abrupt transition to a Snowball Earth state, for perpetual equinox conditions my terra-planet simulations also show an abrupt transition, namely from the HD state to the CW state. These two states exist for low background surface albedo  $\alpha$ , while for high  $\alpha$  only the CW state is possible. The abrupt transition occurs when in the HD state  $\alpha$  is increased beyond a particular threshold value. Moreover, I notice that in my set-up the terra-planet exhibits an open hysteresis: even with background surface albedo reduced to zero it does not return to the HD state. To confirm that the two climate states of the terra-planet are not an artifact of convective parameterizations, I performed an additional simulation with a different convection scheme. By default, the model uses the Nordeng convection scheme (Nordeng, 1994). I have replaced the default settings and simulated terra-planet simulations with the Tiedtke convection scheme (Tiedtke, 1989) and I find the two drastically different climate states irrespective of the convection scheme (figure not shown).

Concerning the global water cycle, the HD and CW states share one important similarity, namely a strong atmospheric moisture flux from low to high latitudes. The planetary boundary layer at low latitudes is extremely dry in the HD state with relative humidity of about 15 %. Clearly, trade winds can maintain such a dry boundary layer only if the water supply at the surface is sufficiently limited. However, without any evapotranspiration at the surface the Hadley cell would dry out completely, losing the greenhouse effect that sustains the high temperatures of the HD state. Furthermore, in the CW state, to keep the rain along the equator one also needs a considerable water supply in the low latitudes. In summary, both climate states are associated with a strong atmospheric transport of water from low to high latitudes, which has to be balanced by evapotranspiration at the low latitudes. Therefore, allowing for both states to be potentially realized under the same boundary conditions, on a real planet, mechanisms must exist that can continuously restore water back to low latitudes. For present-day Earth this happens via the oceans. For the terra-planet in my study water is stored in frozen form at high latitudes like in the past glacial states of our Earth. The resupply of

water may happen via processes like melting of glaciers, transport of ice by gravity flows, and melting at the bottom of large ice caps due to high pressure and geothermal heat flux. This provides liquid water, which may be brought back to the low latitudes by rivers (Abe et al., 2011; Leconte et al., 2013). Note that the huge differences in climate between the two states is primarily a consequence of the completely different functioning of the global hydrological cycle, so that the assumed recycling mechanism can be considered as an additional degree of freedom to the internal dynamics, extending the range of possible terra-planet climates.

My findings may have some relevance for estimates of the habitable zone for such Earth-like terra-planets. In the HD state liquid water is confined to the mid-latitudes (40–50°) in both hemispheres, whereas in the CW state, there is sufficient precipitation and high enough temperatures for permanent liquid water at low latitudes (40° S–40° N). Thus in both climate states life can potentially persist. At the outer edge of the habitable zone, the assumed resupply of water from high to low latitudes stabilizes the greenhouse effect, keeps the planet in the HD state, and may prevent a situation with all water accumulated at the high latitudes in the frozen form. At the inner edge of the habitable zone, by this resupply the planet can maintain precipitation and high cloud cover at the equator in the CW state. Thereby, the planetary albedo is increased, which cools the planet and may prevent the runaway greenhouse state with all the water well mixed in the atmosphere in the gas phase. On the whole, my study thus suggests that the presence of a mechanism which recycles water from the high latitudes back to the low latitudes results, as described, in the two drastically different climate states and may extend the habitable zone of Earth-like terra-planets at low obliquities.



# 4

## Mechanisms behind the planetary scale climate bifurcation on Earth-like Terra-planets

Terrestrial planets like Earth can experience two kinds of planetary scale climate bifurcations: The moist greenhouse bifurcation to a very hot moist greenhouse state by evaporation of all planetary water bodies (Goldblatt et al., 2012; Wolf et al., 2014; Popp et al., 2016) and the Snowball bifurcation to a completely ice/snow covered state (Snowball state) owing to the positive snow-albedo feedback (Budyko 1969; Sellers 1969; Voigt et al., 2010). In addition to these bifurcations, in chapter 3, I demonstrated for water-limited terrestrial planets (terra-planets) at perpetual equinox conditions in the presence of an effective overland water recycling mechanism the possibility of a third type of planetary-scale climate bifurcation that I call Terra-planet bifurcation – leading from a “hot and dry” (HD) climate state to a “cold and wet” (CW) climate state. In this chapter, I discuss the physical mechanisms underlying this bifurcation.

### 4.1 Revisiting the terra-planet bifurcation identified in chapter 3

Figure 4.1 shows the bifurcation diagram (temperature response to changes in soil surface albedo) for the terra-planet from chapter 3. For high soil surface albedo ( $\alpha$ ) (or low solar irradiation), only the CW climate state exists, whereas for low  $\alpha$  (or high solar irradiation), both the HD and CW climate states are stable. Starting in the HD state, upon increasing  $\alpha$  (decreasing solar irradiation) beyond a critical threshold, the terra-planet undergoes an abrupt shift to the CW state. But, starting from the resulting CW state and reversing the forcing (decreasing  $\alpha$  or increasing solar irradiation), the HD state is not restored even for a substantial decrease in  $\alpha$  below the bifurcation point so that the system behaves hysteretic but without the hysteresis being closed (see Fig. 4.1). In the following sections the detailed mechanisms responsible for the bifurcation will be discussed.

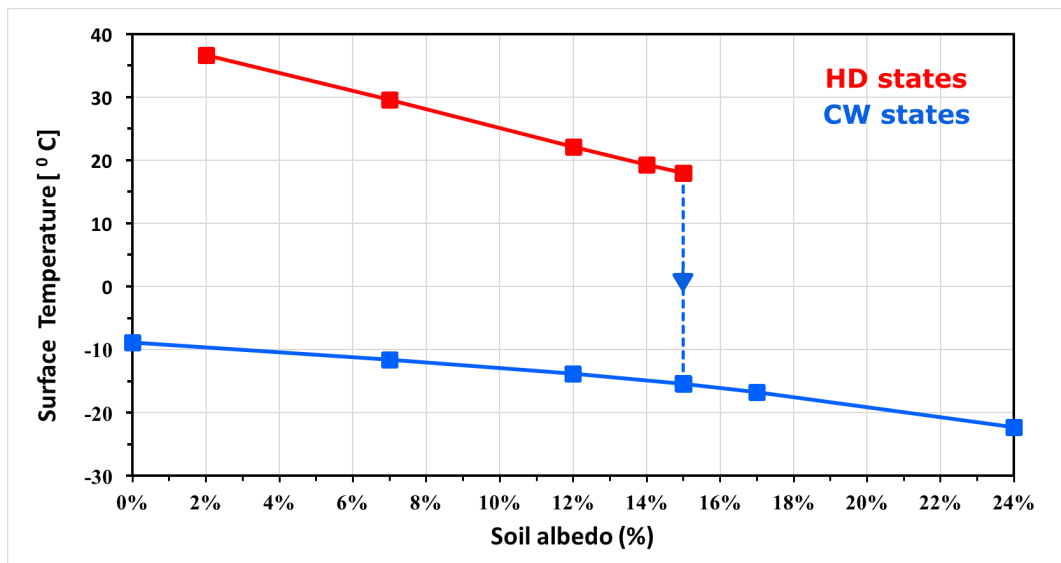


**Figure 4.1** Hysteresis diagram showing the response of the surface temperature to changes in soil surface albedo from chapter 3. At low soil surface albedo ( $\alpha$ ) (high solar irradiation), the terra-planet shows two alternative climate states, a hot and dry (HD) state (red) and a cold and wet (CW) state (blue). When increasing  $\alpha$  (decreasing solar irradiation), above a critical threshold value, the HD state undergoes an abrupt transition to the CW state (dashed line), and further on only the CW state exists. Starting from the CW state at high  $\alpha$ , upon lowering  $\alpha$  (increasing solar irradiation) the planet stays in the CW state even below the point where the HD state collapses. Squares indicate albedo values where states are known from simulations. The surface temperature values are obtained from simulations with ICON-ESM for zero obliquity condition (Z2-Z24, TRANS simulations in Table 2.1)

Transitions between alternate stable states can occur either due to natural fluctuations or due to external perturbations (Scheffer et al., 2001). In the presence of multistability, both factors can potentially push the planet away from its steady state. Considering small perturbations of a stable state, negative feedbacks inherent to the system bring back the system to its original state. However, in the presence of multistability larger perturbations can initiate positive feedbacks that overpower the stabilizing negative feedbacks and may drive the system from one stable state to another. Hence, in order to get a complete understanding of the driving mechanisms of a bifurcation, one needs to examine both the negative feedbacks that keep the individual climate states stable and the positive feedbacks that can trigger the transition between them. Accordingly, this chapter addresses the following questions:

- What mechanisms keep the two different terra-planet climate states stable?

- Why does the HD state collapse? What is the essential mechanism to initiate the transition to the CW state?
- Why does the terra-planet system show hysteretic behaviour?

This chapter is structured as follows: In Section 4.2, I summarize the general characteristics of the two climate states and review the characteristics of the Terra-planet bifurcation. Here, I highlight in particular those characteristic differences between the two climate states that are crucial for understanding the stabilizing/de-stabilizing mechanisms of the individual states. In Section 4.3, I describe the perturbation experiments that I performed for understanding the stability of the HD state and discuss the negative feedback that stabilizes the HD state. In Section 4.4, I discuss the reasons why this stabilizing negative feedback mechanism fails so that the transition to the CW state is initiated. In Section 4.5, I discuss the negative feedback that stabilizes the CW state and turns out to be responsible for the hysteretic behaviour.

## 4.2 Characteristics of the Terra-planet bifurcation

The occurrence of the Terra-planet bifurcation depends on the following two conditions: Firstly, the presence of an effective overland water recycling mechanism. Generally, water evaporates from the warmer regions of a planet and gets accumulated at the colder regions by the atmospheric circulation. On water-dominated planets, this water accumulated at the colder regions is transported back to the warmer regions via ocean currents. However, on water-limited planets (terra-planets), the recirculation of water can occur only through river or subsurface flows in the soils and I refer to this recycling mechanism as the *overland water recycling* (chapter 3). Technically, this is achieved in my terra-planet simulations by assuming a kind of subsurface ocean embedded in the soils held at a constant minimum water level. This subsurface ocean mimics the recirculation of water back to the warmer regions, as oceans do on Earth except that it implies a higher resistance to evaporation due to the presence of soils.

The second condition for the appearance of the Terra-planet bifurcation is the existence of two alternative climate states – a “hot and dry” (HD) state and a “cold and wet” (CW) state in the presence of the above mentioned overland water recycling. They turn out to differ drastically in terms of their global mean temperature, low-latitude water cycle, moisture distribution and, mean circulation pattern (see chapter 3).

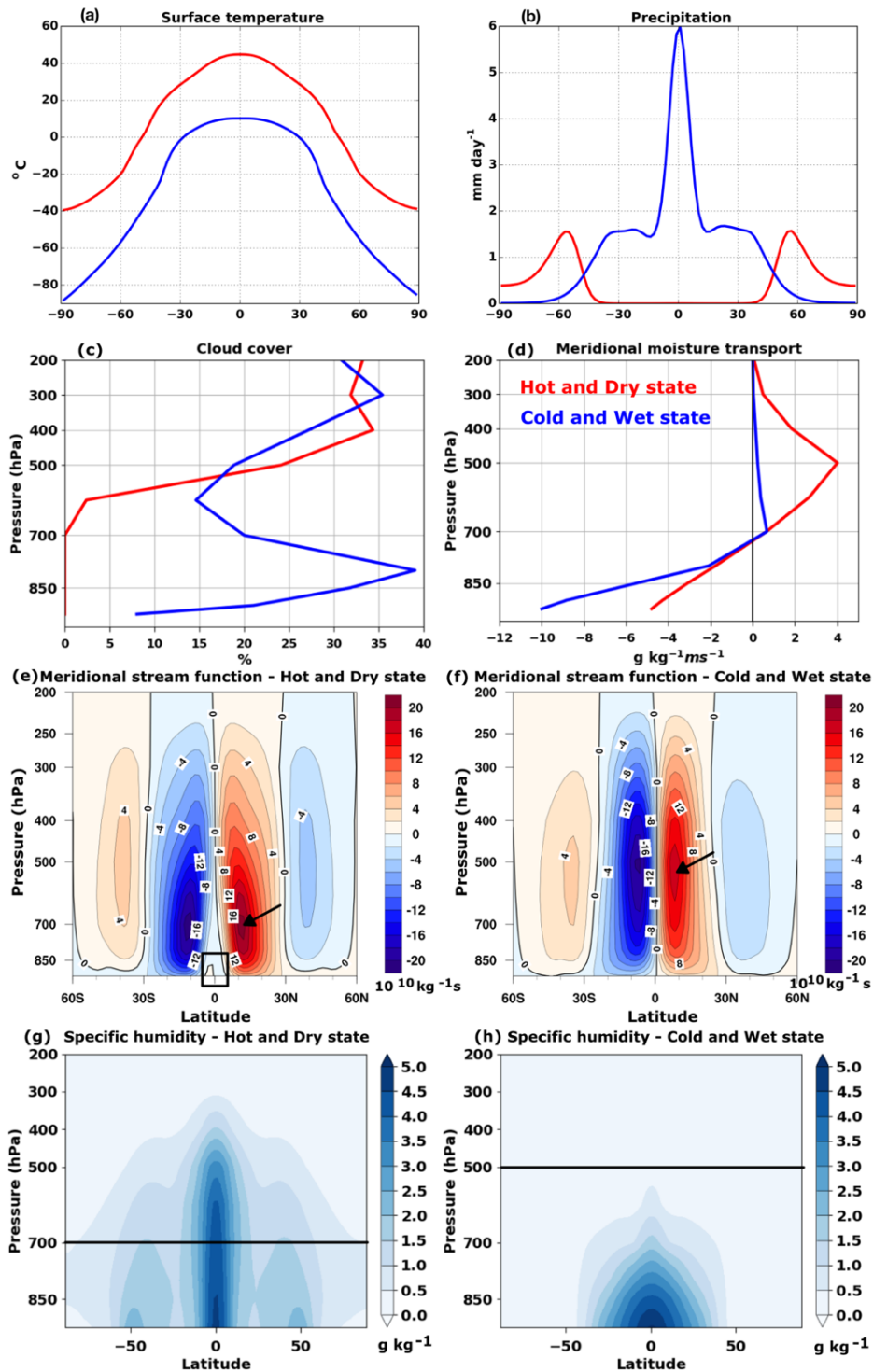


**Figure 4.2** (a, b) Annual mean meridional profiles of surface temperature and precipitation, (c, d) vertical profiles of cloud area fraction averaged over the low latitude region (30°S - 30°N) and meridional transport of water at 10°N, (e, f) meridional stream function in  $10^{10} \text{ kg s}^{-1}$ , (g, h) specific humidity in  $\text{g kg}^{-1}$  for the HD ( $\alpha = 0.14$ ) and CW ( $\alpha = 0.15$ ) climate states corresponding to the simulations Z14 and Z15 in Table 2.1. The black arrows in (e) and (f) and black lines in (g) and (h) denote the location of the northern Hadley circulation centre. The black box in (e) denotes the reverse secondary circulation cell (5°S - 5°N). Red/Blue lines refer to HD/CW states.

The major difference between the two climate states that is relevant for the following discussion on the stability of the different climate states is, where the majority of the moisture is present in relation to the Hadley cell centre. In the HD state majority of the moisture is present in the upper branch of the Hadley cell whereas in the CW state majority of the moisture is present below the Hadley cell centre.

The CW state is characterized by low temperatures (Fig. 4.2a) and lower saturation water vapour pressures in the low-latitude region. Lower saturation water vapour pressure facilitates condensation and cloud formation at lower tropospheric levels (Fig. 4.2c). These low clouds have high liquid water content so that rain drops are large enough to produce intense precipitation in the low-latitude region of the CW state (Fig. 4.2b). The Hadley circulation in the CW state has a high centre with poleward winds in the upper troposphere like in the present-day Earth (Fig. 4.2f). Most of the moisture in the CW state is precipitated and recycled within the low-latitude region and very less moisture is present in the upper branch of the Hadley cell to be exported to the high latitudes (Fig. 4.2h).

Instead, the HD state is characterized by very hot temperatures in the low-latitude region (Fig. 4.2a), which means extremely high saturation water vapour pressures as a consequence of the Clausius-Clapeyron relation. Despite also extremely low relative humidity in the lower troposphere the absolute atmospheric moisture content is relatively high at the equator (on average about  $4 \text{ gkg}^{-1}$  up to 500 hPa) compared to the CW state (Fig. 4.2g). In such a terra-planet atmosphere, condensation and cloud formation take place only in the upper part of the troposphere (Fig. 4.2c). These high clouds have low liquid water content so that rain drops are small and can occur only in form “virga rain”, i.e. the rain droplets evaporate somewhere below the cloud base in the hot and dry air (around 500 - 700 hPa) before reaching the ground. For the following it is important to note that the cooling induced by the evaporation of virga rain modifies the local vertical stability of the atmosphere: in the upper part of the layer where the evaporation of virga occurs, the vertical stability is increased, whereas the lower part of this layer is destabilized. I refer to this upper part of layer as the ‘stable layer’ and for the HD state in stable conditions, it is formed at mid-tropospheric levels so in the discussion corresponding to HD state stability, it is also referred to as the ‘mid-tropospheric stable layer’. The cold air descending from the destabilized layer drives a small ‘reverse secondary circulation cell’ close to the equator [ $5^{\circ}\text{S}$  to  $5^{\circ}\text{N}$ ] (Fig. 4.2e).

Commonly the poleward winds that form the upper branch of the Hadley cell only occur in the upper troposphere and transport only minor amounts of moisture like in the CW state. By contrast, in the HD state poleward winds also develop at the stable layer due to the evaporative cooling in the mid-troposphere (at around 500 hPa, Fig. 4.2e) resulting in a low-centred Hadley cell. These poleward winds transport high amounts of moisture (Fig. 4.2d) as they form close to the cloud base (i.e. close to saturation) and at much higher temperature than in the upper troposphere. Export of moisture out of the low-latitude region sustains a high vapour pressure deficit (VPD) in the low-latitude region of the HD state.

For the following discussion about the stability of the climate states, the stable layer, reverse secondary circulation cell and poleward moisture transport at the mid-tropospheric levels is very crucial.

### 4.3 Stability of the HD state

In this section I explain, why the HD state is stable for small values of soil surface albedo. To discuss the stability of a particular state, one has to consider the response of the system to small perturbations. In principle, the HD state is stable against all types of weather anomalies. Since the major aim in this chapter is to understand how the terra-planet bifurcation gets possible, I concentrate only on stability against VPD anomaly, because such an anomaly turns out to be relevant to the bifurcation. As mentioned in the second section, the main distinction in the functioning of the two states is a result of a huge difference in temperature and moisture conditions at low latitudes. Therefore, I consider only a hypothetical cold/wet anomaly in the troposphere of the low-latitude region in the HD state with the main consequence of a lower than usual VPD below the cloud base. The mechanism to be explained is depicted in Fig. 4.3. At the height of the hypothesized VPD anomaly, moisture is transported with the upper branch of the Hadley cell to higher latitudes. A small decrease in VPD at this height results in a drop in the cloud condensation level (the response is positive). A lower cloud condensation level leads to a lowering of the height at which the evaporation of “virga” occurs. This in turn decreases the height of the mid-tropospheric stable layer and lowers the height of the poleward moisture transport. Accordingly, the temperature at this stable layer is higher than it would be without the vertical shift. Since the stable layer is located close to the cloud base (see section 4.2), it is always close to saturation. Together with the higher temperature this

implies that more moisture is transported at this stable layer to higher latitudes, which results after some time in an increase in VPD in the low-latitude region. Thus, the initial negative anomaly in VPD is dampened by this negative feedback mechanism, which stabilizes the HD state.

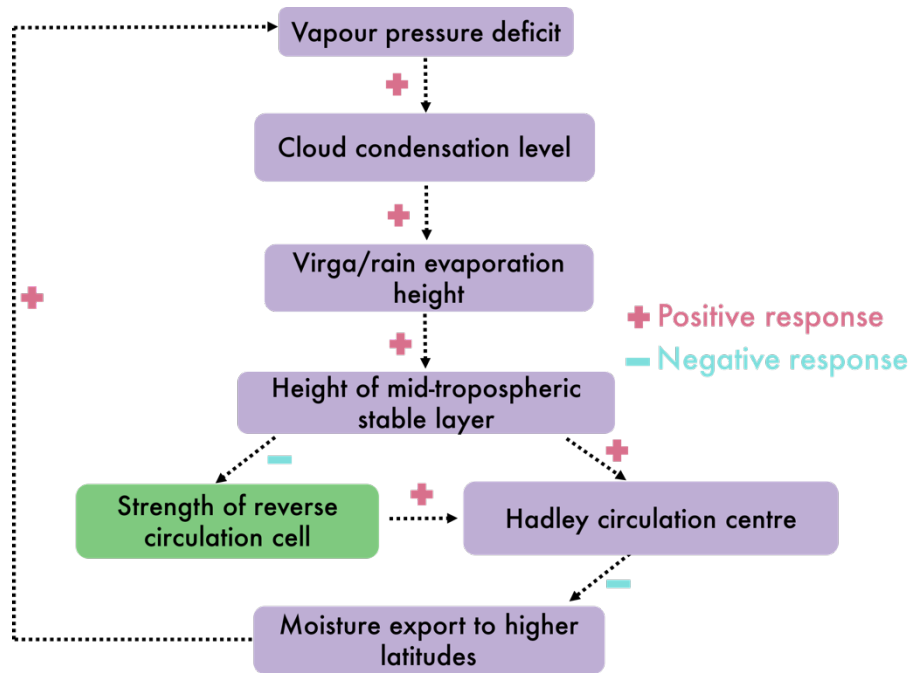


**Figure 4.3** Low latitude feedback stabilizing the HD state for small perturbation (purple boxes) and destabilizing the HD state for larger perturbations when the mechanism indicated in the green box turns the negative feedback into positive feedback. More explanations are given in the text in Sect 4.3.

#### 4.4 Transition from the HD state to the CW state

The existence of two drastically different climate states implies that there is at least one bifurcation point. The bifurcation point is out of the range of normal weather fluctuations in HD simulations with soil surface albedo  $\alpha$  less than 0.15, because these simulations (see Fig. 4.1) persist in the HD state for many years. By increasing  $\alpha$  to 0.15, the average climate state is shifted slightly towards the bifurcation point, e.g. the global mean surface temperature decreases by 1.4 K and, a transition from the HD state to the CW state randomly begins after several years. Accordingly, an extreme weather anomaly is necessary to initiate the transition, i.e. to reach the bifurcation point.

In view of the negative feedback stabilizing the HD state, one of the response signs in the feedback diagram in figure 4.3 has to reverse sign to initiate the transition. This

happens when an anomaly has lowered the mid-tropospheric stable layer very low in the troposphere that any further descent of this layer would decrease the poleward moisture transport instead of strengthening it i.e moisture is no longer transported polewards via the upper branch of the Hadley cell but gets trapped by the lower branch in the low-latitude region is located. In the following I explain how the sign in the feedback diagram is reversed in detail:

Assume a large drop in VPD in the low-latitude region which shifts the cloud condensation level to the lower troposphere (much lower than the 600 hPa level, which is the usual minimum height of clouds in the HD state, Fig. 4.2c). This would be accompanied by a considerably lower evaporation height of virga. Suppose the weather anomaly is very strong that the rain drops almost reach the ground. The majority of rain evaporation would then occur in the trade wind convergence zone (below 800 hPa). This would lower the stable layer developed due to evaporative cooling also into the trade wind convergence zone where moisture is transported with the lower branch of the Hadley cell. Accordingly, the poleward winds formed at the stable layer are directed against the equatorward propagating trade winds. This is weakening the poleward moisture transport at mid-tropospheric levels. In Fig. 4.4 this sets in at around day 300 for the meridional section 0-50°E. I specifically consider this meridional section because it is the region where the first precursors of the transition appear and the precipitation reaches the ground for the first time. From now on, the discussion is only based on this particular meridional section (0-50°E) until the precipitation reaches the ground.

A lower VPD implies also a higher rain production rate, meaning more evaporative cooling in the trade wind convergence zone. In the lower portion of the layer, where the virga rain evaporates, the additional cooling destabilizes the atmosphere further leading to stronger descending motion (see Sect. 4.2). As a consequence, the reverse low level circulation cell in the HD state (Fig. 4.2e) is strengthened during the onset of the transition (in the meridional section 0-50°E). The secondary cell expands from the equator to about 15° latitude for about one year starting from around day 360 (Fig. 4.4a) and intensively circulates water vapour: poleward close to the surface and equatorward at about 800 hPa.

At the same time the vertically integrated poleward moisture transport at 10° latitude decreases and becomes negative (Fig. 4.4b). This is a clear indication that the sign in the feedback diagram (Fig. 4.3) has switched. Essentially, this happens, because poleward winds at mid-tropospheric levels are further diminished from day 360 (Fig.

4.4a). In contrast to the HD state there is no midlevel poleward moisture transport at about 600 hPa anymore. It now only occurs in the higher troposphere (around 500 hPa) and is weaker compared to the HD state (Fig. 4.4). The reason is the expansion and strengthening of the secondary cell, which elevates the position of the usual equatorward winds by about 200 hPa and thereby diminishes the poleward mid-level winds below 500 hPa. Accordingly, the moisture convergence associated with the lower branch of the Hadley cell is no longer compensated by a poleward midlevel flow like in the HD state. In summary, the vertical integral of meridional moisture transport in the low-latitude region becomes negative that implies an accumulation of moisture in the troposphere of the low-latitude region (Fig. 4.4c), which results in precipitation at the surface after sometime at around day 500 in the meridional section 0-50°E (Fig. 4.5).

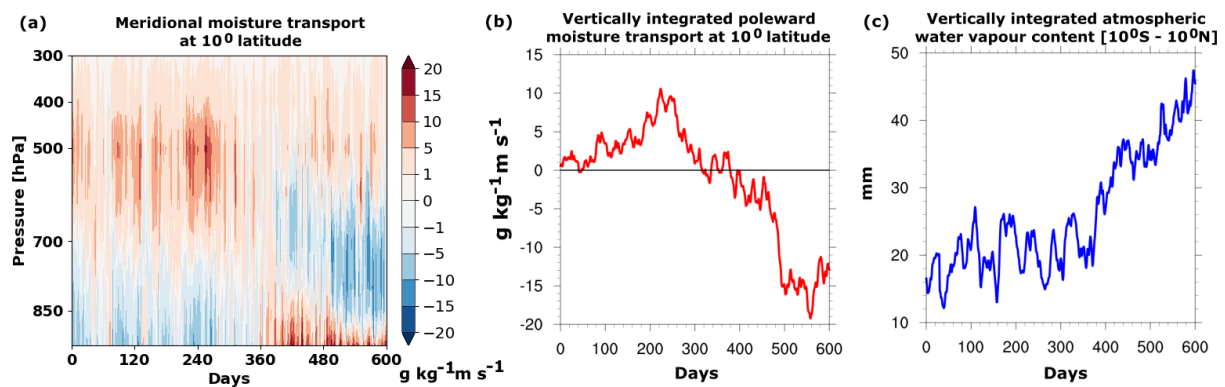


**Figure 4.4** Time evolution during the transition from the HD to the CW state at the bifurcation (simulation TRANS in Table 2.1). The figures show the behaviour in the meridional section 0-50°E only, because the transition happens at different times in different sections. (a) Meridional moisture transport at 10° latitude (averaged over both hemispheres), (b) Vertically integrated meridional moisture transport at 10° latitude (averaged over both hemispheres), (c) Vertically integrated atmospheric water vapour content in the low-latitude region (10°S to 10°N). The transition to the CW state begins randomly about 12 years after the increase in soil surface albedo is applied. The plot here shows the time evolution in days starting from year 11. In (a, b) positive values indicate poleward transport and negative values indicate equatorward transport.

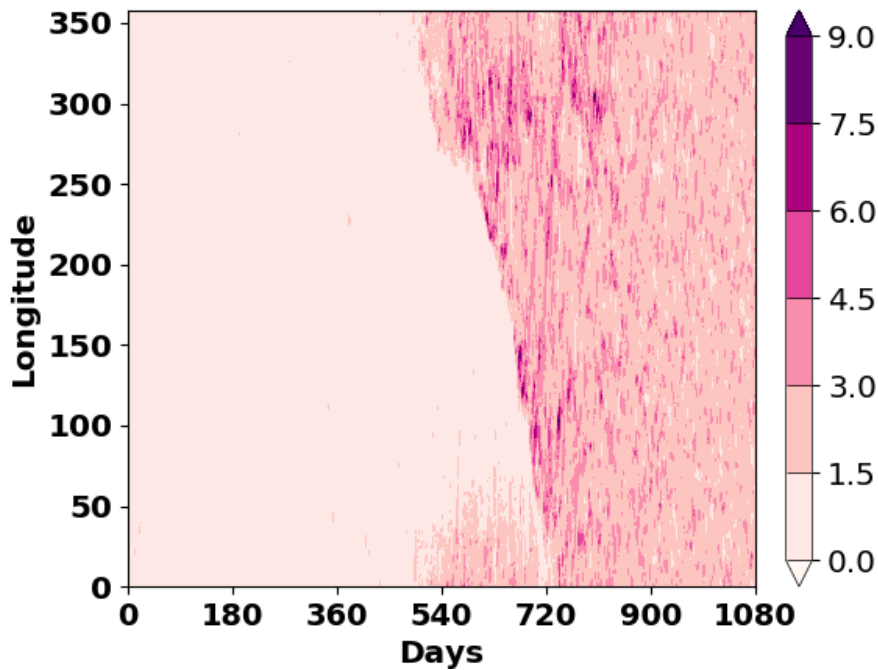


*Figure 4.5* Time evolution of surface precipitation ( $\text{mm day}^{-1}$ ) in the low-latitude region during the transition from HD state to CW state (simulation “TRANS” in Table 2.1). The transition to the CW state begins in this simulation randomly 12 years after the increase in soil surface albedo is applied in the HD state. The plot shows the time evolution in days starting from year 11. Around day 500, the precipitation reaches the ground in the low-latitude region and starts spreading westward eventually resulting in the zone of intense rain similar to the ITCZ on present-day Earth.

With precipitation reaching the ground in the low-latitude region it initiates a series of positive feedbacks: The moisture in the uppermost soil layers’ increases. Increase in soil moisture increases the evaporation at the surface. Increase in evaporation at the surface increases the amount of moisture available for condensation in the lower troposphere. Increase in moisture availability leads to an increase in latent heat release due to condensation. Increased latent heat release promotes stronger rising motion of air and thereby results in a stronger Hadley circulation that promotes stronger convection and intense precipitation – this is a self-amplifying positive feedback.

Shortly after the precipitation reaches the ground in the low-latitude region, it continues to spread westward to the neighbouring regions along with the prevailing easterlies in the low-latitude region eventually resulting in the formation of a region of intense precipitation (Fig. 4.5). This region of intense precipitation resembles the

Intertropical convergence zone (ITCZ) observed on present-day Earth. The spreading of the precipitation around the low-latitude region occurs due to moisture advection by the westward propagating easterlies.

Substantial increase in moisture convergence in the low-latitude region causes an increase in cloud cover and in turn an increase in planetary albedo (Fig. 4.6a). This further accelerates the global mean cooling allowing snow cover to advance to lower latitudes down to  $40^\circ$  (Fig. 4.6b). Together, expansion of snow-cover to low-latitudes and a reduced poleward moisture transport confine the rain bands to the low-latitude region (Fig. 4.6c).

#### 4.5 Stability of the CW state

In this section I describe mechanisms that keep the CW state stable. In particular, I want to understand, why the CW state cannot be reverted to the HD state by lowering the albedo. For this purpose, I consider only perturbations potentially apt for triggering a transition towards the HD state. Hence, I consider only a hypothetical local dry/heat anomaly in the troposphere at the equator in the CW state.

A local dry anomaly would decrease the rain rate in that region and reduce the accumulation of water at the surface given by precipitation minus evaporation there. However, the trade winds would continue to transport atmospheric moisture at the same rate to the equator like in the situation without the local anomaly. Most of this accumulated moisture at the equator has to be precipitated after some time because: In the CW state, poleward moisture transport occurs only at higher altitudes and at these high altitudes, the poleward flowing air is characterised by low water vapour saturation pressure associated with only minor poleward moisture transport. Furthermore, the dry anomaly at the equator cannot initiate poleward moisture transport at mid-tropospheric levels because the lower troposphere is too cold to cause strong virga rain evaporation and lead to a mid-tropospheric stable layer that would be necessary to initiate the mid-tropospheric poleward transport. Therefore, due to mass conservation of water the continuing moisture convergence by the trade winds will stabilize the precipitation at the equator and restores the precipitation rate to the value before the anomaly.

Similarly, consider a small warm anomaly in the low-latitude region of the CW state. Accordingly, the cloud base would raise and the fraction of rain drops evaporating below the clouds would increase. However, the absolute moisture content of the atmosphere and the low-level moisture convergence by the trade winds would be kept

unaltered. Following the same arguments as in the case of a dry anomaly this enforces the precipitation to continue at the same rate at the equator. Meanwhile, the warm anomaly is advected by the upper branch of Hadley cell circulation to higher latitudes and dissipated there via outgoing longwave radiation.

Of the two anomalies considered, the warm anomaly has more potential to stop the precipitation in the low-latitude region and initiate a transition to the HD state because the warm anomaly shifts the atmospheric conditions at the equator directly towards those realized in the HD state (i.e. increase in evaporation of rain drops). By contrast, the dry anomaly is just temporarily reducing the precipitation rate without any potential to change the Hadley cell circulation structure.

Therefore, if we assume a hypothetical strong warm anomaly that is spatially more extended in the equatorial region, the anomaly could in principle stop the precipitation there: The VPD in the lower troposphere of this region have to increase which might lead to increased evaporation of virga rain and thereby the development of a stable layer causing moisture to be transported poleward in this mid-tropospheric layer. However, as seen in Fig. 4.5 between day 580 and day 720, the easterlies would advect atmospheric conditions from the neighbouring region and initiate precipitation in the heated region again.

In summary, the transition from the HD state to the CW state may be initiated locally at the equator whereas the transition from the CW state to the HD state could only be started by a drastic large scale change in the equatorial region: the atmosphere of the equatorial region has to be warmed by about 20 K to sufficiently increase VPD, to inhibit precipitation along the whole low-latitude region, to form a mid-tropospheric stable layer and to promote poleward moisture transport. I see this as the reason for the hysteretic behaviour of the terra planet (Fig. 4.1).

## 4.6 Summary

*Stability of the HD state:* Complete evaporation of rain drops keeps the HD state stable. Evaporative cooling creates a stable layer at mid-tropospheric levels. This stable layer generates poleward winds at mid-tropospheric levels. The poleward winds lead to an enhanced moisture transport out of the low-latitude region and thereby inhibit rain in the low-latitude region of the HD state.

*Processes leading to initiation of precipitation in the low-latitude region:* A stronger than usual weather anomaly causing moister conditions in troposphere of the low-latitude region could lead to more evaporative cooling at lower tropospheric levels and a strengthening and deepening of the reverse circulation cell. This diminishes the poleward midlevel winds at mid-tropospheric levels. As a consequence, moisture accumulates in the troposphere of the low-latitude region and leads to initiation of precipitation there.

*Reason for hysteresis:* while the transition from the HD state to CW state can be initiated by local hydrological feedbacks, for the transition from CW state to HD state to occur the atmospheric temperatures in the low-latitude region should increase by about 20K to inhibit the intense precipitation there. This would not be possible with just a decrease in soil surface albedo since the high cloud cover in the CW state shields the surface from solar irradiation and the reduction of soil surface albedo has only a minor effect on the atmospheric temperatures.

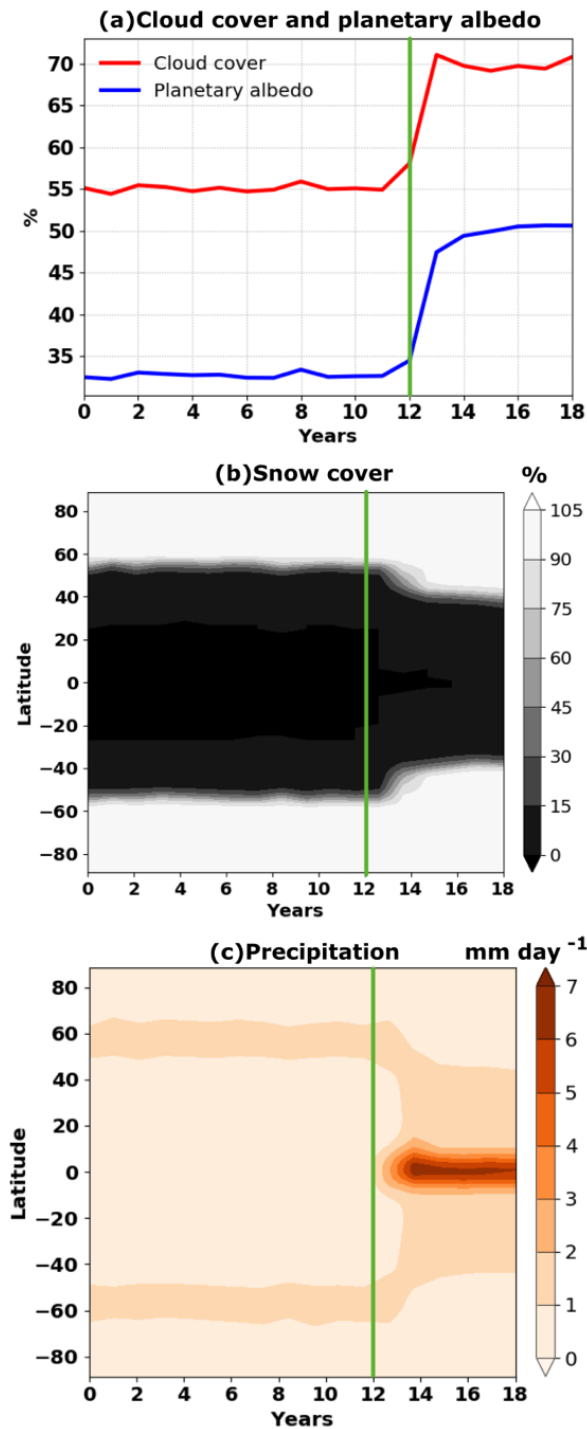


Figure 4.6. Time evolution of (a) cloud cover and planetary albedo, (b) snow cover (%) (c) precipitation ( $\text{mm day}^{-1}$ ) during transition from HD state to CW state (simulation "TRANS"). The transition to the CW state begins randomly 12 years (denoted by green vertical lines) after the increase in soil surface albedo is applied in the HD state. With the increase in moisture convergence in the low-latitude region, cloud cover and planetary albedo increase resulting in the shift of snow cover and rain bands to low-latitudes

# 5

## The effect of obliquity on the climate of terra-planets

In this chapter, I analyse whether for non-zero obliquities, a transition from the HD to CW climate state similar to the one reported in *chapter 3* can be realised. I do this using a set of idealised simulations with the ICON climate model in terra-planet configuration. I would like to point out that this chapter is mainly descriptive and limited to finding a possible abrupt climate transition for non-zero obliquities.

### 5.1 Three drastically different climate states with non-zero obliquity

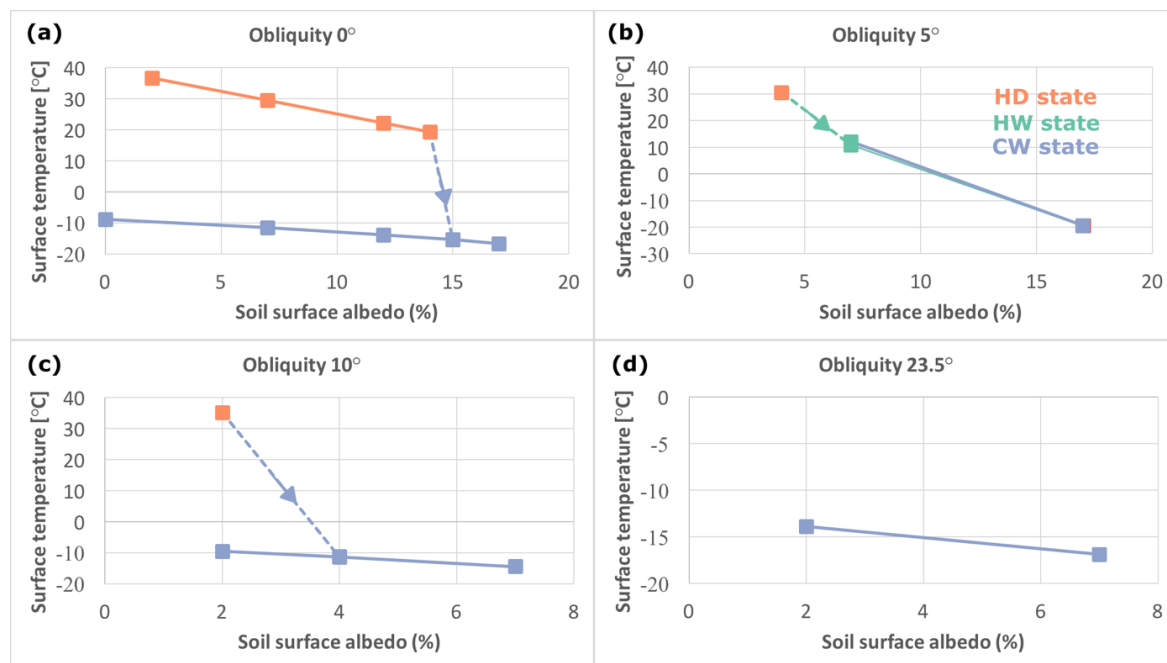


**Figure 5.1** Global mean surface temperature as a function of soil surface albedo ( $\alpha$ ) for obliquity (a)  $\varnothing = 0^\circ$ , (b)  $\varnothing = 5^\circ$ , (c)  $\varnothing = 10^\circ$ , (d)  $\varnothing = 23.5^\circ$ . Dotted lines denotes the spontaneous transition from HD to CW in (a,c) and transition from HD to HW state in (b) when increasing  $\alpha$ . From  $\varnothing = 0^\circ$  to  $10^\circ$  (a,c), the range of  $\alpha$  values for which the terra-planet is bi-stable is reduced. At  $\varnothing = 23.5^\circ$  (c), the terra-planet is mono-stable. No bistability is found for  $\varnothing = 5^\circ$  (b). The data for the figure is obtained from the S2-S17 simulations in Table 2.1 (see chapter 2)

Fig. 5.1 shows the surface temperature response for different terra-planet simulations to varying soil surface albedo values for seven different obliquities ( $\emptyset$ ) varying from  $0^\circ$  to  $23.5^\circ$ . Depending on the value of obliquity, the terra-planet can either exhibit two or three different climate states: For  $\emptyset < 5^\circ$  and  $10^\circ \leq \emptyset < 23^\circ$ , the terra-planet exists in two climate states: Hot and Dry (HD) state and Cold and Wet (CW) state. Whereas, for  $5^\circ \leq \emptyset < 10^\circ$ , the terra-planet exhibits an additional climate state that I refer to here as the 'Hot and Wet' (HW) state in addition to the HD and the CW climate states. The three terra-planet states display drastically different climates.

As the obliquity is increased, the range of soil albedo values for which the HD state is stable is reduced. The largest extent of HD state (i.e., largest range of soil surface albedo values for which HD state is stable) is observed for low obliquity ( $0^\circ$ ) (Fig. 5.1 a-d). The intermediate HW state is only stable for intermediate obliquities  $5^\circ \leq \emptyset < 10^\circ$ . The largest extent of CW state is observed for present-day Earth's obliquity.

## 5.2 Mean climate of the Hot and Wet (HW) state

Since the climate characteristics of the HD and CW states were already explained in chapters 3 and 4. Here, I only discuss the details about the climate of the new HW state and compare it with the climate of HD and CW states. The HW state is characterised by a hot climate with an intense low-latitude precipitation. The global mean surface temperature in the HW state is around  $10^\circ\text{C}$  and the low-latitude temperatures are around  $30^\circ\text{C}$  (Fig. 5.2a). The high temperatures in the low-latitude region facilitate high evaporation there (Fig. 5.2f). The high evaporation leads to a moist atmosphere (Fig. 5.2d) and in turn strong greenhouse warming. The strong greenhouse warming keeps the HW state hot. The HW state is hotter than the CW state but colder than the HD state (Fig. 5.2a).

Even though the temperatures in the low-latitude region of the HW state are high they are not high enough to lead to "virga rain" and rain evaporation like in the HD state. Instead, the low-latitude region of the HW state is associated with a high amount of cloud cover (Fig. 5.2e) and intense precipitation (Fig. 5.2b) like in the CW state. Furthermore, the net annual mean precipitation in the HW state is more intense compared to the CW state (Fig. 5.2b). The reason is higher evaporation in the HW state leads to an enhanced precipitation (Fig. 5.2f).

The spatial distribution of snow cover in the HW state is very different from that of the CW state (Fig. 5.2c). In the HW state, snow cover fraction is confined to the higher

latitudes up to  $50^\circ$  while, in the CW state, it reaches much lower latitudes (up to  $40^\circ$  latitude). Also the cloud cover distribution varies between the CW and HW states especially in the sub-tropical region ( $20^\circ - 30^\circ$  latitudes) (Fig. 5.2e). The HW state supports much lower cloud cover in the sub-tropics compared to the CW state.

Figure. 5.3 shows the northward transport of total energy for the three climate states at 0, 5, 10 obliquities and soil surface albedo 0.07. The total northward energy transport for the HW state is larger than in the HD and the CW states. Larger northward energy transport in the HW state results in a smaller equator-to-pole temperature gradient preventing the snow cover to advance equatorward in contrast to the CW state where snow cover is present upto  $40^\circ$  latitude (Fig. 5.2c). Overall the climate in the HW state is milder than the CW state and closer to the present-day climate.

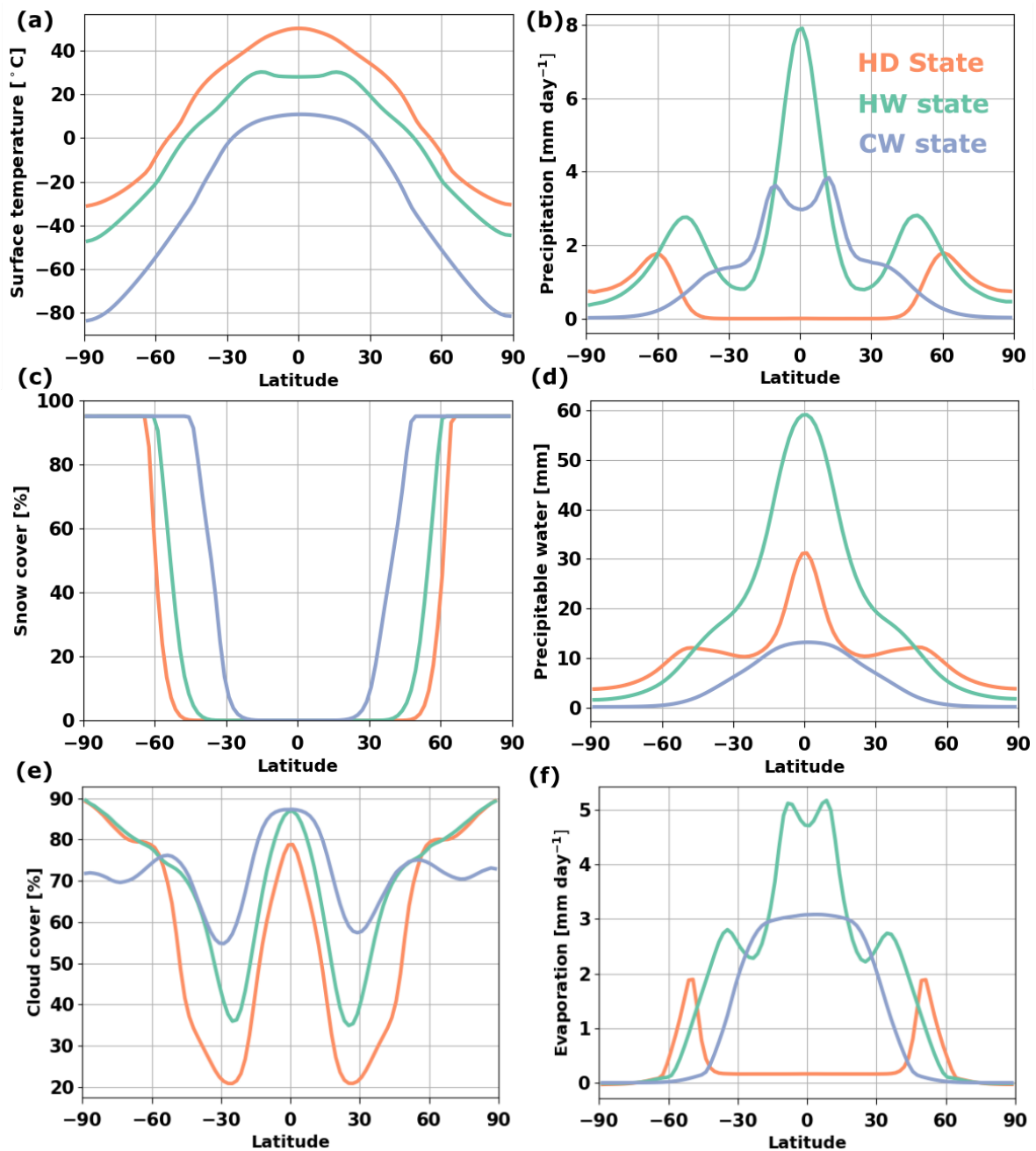


**Figure 5.2** Annual mean meridional profiles of (a) surface temperature, (b) precipitation, (c) snow cover, (d) precipitable water, (e) cloud fraction, and (f) evaporation for the three terra-planet states: HD, HW and CW for the simulations with soil surface albedo of 0.07 and obliquities  $0^\circ$ ,  $5^\circ$  and  $10^\circ$  respectively.

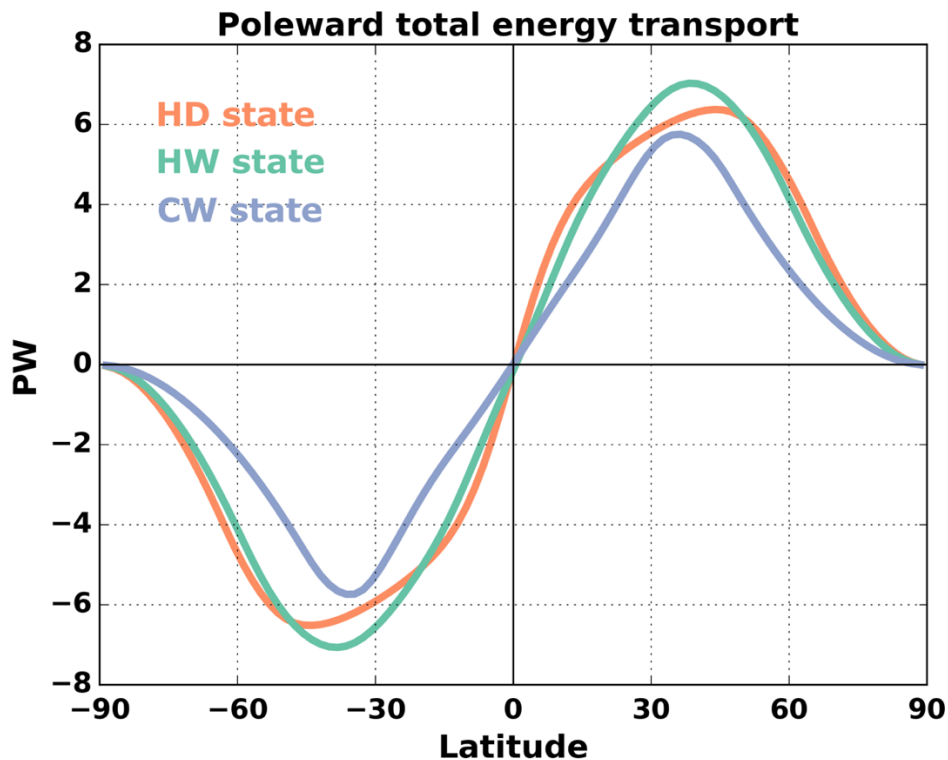


*Figure 5.3 Annual mean behaviour of northward transport of total energy in petawatts (PW) for the three terra-planet states: HD, HW and CW for the simulations with soil surface albedo of 0.07 and obliquities  $0^\circ$ ,  $5^\circ$  and  $10^\circ$  respectively.*

### 5.3 Two different climate instabilities with non-zero obliquity

Two different abrupt climate transitions are realised for a terra-planet with varying soil albedo values and a seasonal orbit: “transition from HD state to CW state” and “transition from HD state to HW state”.

#### 5.3.1 Abrupt transition from HD state to CW state

For  $\varnothing < 5^\circ$  and  $10^\circ \leq \varnothing < 23^\circ$ , abrupt transition from the HD state to the CW state occurs when the soil surface albedo in the HD state is increased beyond a critical threshold value similar to that discussed in chapter 3 (Fig. 5.1 a, c). However, the critical threshold value of soil surface albedo at which the abrupt bifurcation to the CW state occurs is lowered with the increase in obliquity from  $\alpha = 0.15$  for zero obliquity to  $\alpha = 0.04$  for  $\varnothing = 15^\circ$  (Fig. 5.1c).

### 5.3.2 Abrupt transition from HD state to HW state

For  $5^\circ \leq \varnothing < 10^\circ$ , a second abrupt transition from the HD to the new HW climate state occurs when the soil surface albedo in the HD state is increased beyond a critical threshold value (Fig. 5.1b). Preliminary analysis shows that this “abrupt transition to the HW state” is similar to the “abrupt transition to the CW state” – both the transitions lead to an initiation of precipitation in the low-latitude region. However, the cooling resulting from the two transitions is very different. The abrupt cooling associated with the “transition to HW state” is about 20 K lower than the cooling resulting from the “transition to the CW state”. The reason for this difference in cooling is because: the additional cooling in the “transition to the CW state” arises due to the strong snow albedo feedback leading larger areas of snow cover on the planet (Fig. 5.2e). This leads to an enhanced cooling of the planet during the “transition to the CW state”. Whereas, in the HW state the snow-albedo feedback weakened since the large poleward energy transport in the HW state (Fig. 5.3) warms the higher latitudes and prevents the advance of snow cover equatorward (Fig. 5.2e). A weaker snow albedo feedback in the HW state results in smaller snow cover compared to the CW state. This leads to a lower planetary albedo which results in less abrupt cooling for the “transition to the HW state” compared to the “transition to the CW state”.

### 5.3.3 Gradual transition from HW state to CW state

Furthermore, for  $\varnothing = 5^\circ$  starting in the HW state, and increasing the soil surface albedo further beyond 0.07, leads to a slow and smooth transition of climate to the CW state (Fig. 5.1b). With the increase in the soil surface albedo in the HW state, the net radiation at the surface is further reduced. This allows snow cover to slowly advance to the lower latitudes. Consequently, the snow albedo feedback strengthens leading to a further cooling of the planet and resulting in the CW state.

## 5.4 Bistability and hysteresis with non-zero obliquity

For  $\varnothing < 5^\circ$  and  $10^\circ \leq \varnothing < 23^\circ$ , starting in the CW state and lowering back the soil surface albedo beyond the critical threshold does not lead back to the HD state. This indicates a closed hysteretic behaviour for non-zero obliquities similar to that discussed in chapter 3 for zero obliquity (Fig. 5.1a, c).

The bistability reported in chapter 3 is also found for non-zero obliquities: For  $\varnothing < 5^\circ$  and  $10^\circ \leq \varnothing < 23^\circ$ , both HD and CW state are stable for the same boundary conditions. However, the width of the bi-stable region (the range of  $\alpha$  values for which the terra-planet is bi-stable (both HD and CW climate states are stable under same boundary conditions)) is reduced when the obliquity gets larger (Fig. 5.1a,c). And, the bistability is lost at present-day Earth's obliquity (Fig. 5.1d): For  $\varnothing = 23.5^\circ$ , terra-planet is mono-stable – only CW state exists and the HD state is no longer stable even for a very low  $\alpha$  (Fig. 5.1d).

The decrease in the width of the bi-stable region with the increase in obliquity could be due to the seasonal migration of the rain bands towards the low latitudes. The seasonal migration of rain bands facilitates seasonal rain in the dry low-latitude region. Since soil moisture has a memory lasting for several weeks to months, this causes the top soil layers in the low latitudes to remain wet even during the dry season. Thus there is always soil moisture in the originally dry low-latitude region to allow for continuous evaporation and precipitation. This probably destroys the HD state increasing the chances of occurrence of the transition to the CW state. A more detailed study on the reasons behind the loss of bistability for non-zero obliquities is ongoing but beyond the scope of the present study.

## 5.5 No bistability or hysteresis for $\varnothing = 5^\circ$

Starting in the stable HW state at  $\varnothing = 5^\circ$  and lowering back the soil surface albedo below the threshold value until 0 does not result back in the HD state (Fig. 5.1b). It leads to large fluctuations in the system – temperature variations of the order 10K (figure not shown). From preliminary analysis, no stable state could be achieved even when the simulation was run for a long period of time. Even though a stable state could not be achieved, the simulation results indicate active precipitation in the low-latitude region at low soil surface albedo value, this could be considered as a sign for the possibility of bistability between the HD and HW climate state. However, further analysis is needed to confirm the existence of this bistability at  $\varnothing = 5^\circ$  and would be a subject of future work.

Similarly, starting in the stable CW climate state and reversing the forcing (lowering the soil surface albedo below the threshold) results immediately in the HW state (Fig. 5.1b). The snow cover retreats poleward and intensity of precipitation in the

low-latitude region increases again. This indicates that there is no bistability between HW and CW climate states or hysteresis in the system.

## 5.6 Discussion and Conclusions

In this chapter, I explored the influence of seasonal variability on the climate of terra-planets with an effective overland water recycling mechanism. For a range of soil surface albedo values and obliquities in the range of  $0^\circ$  to present-day Earth obliquity value, I find that the terra-planets with a non-zero tilt could stabilise in a diverse variety of climate states. This is in contrary to the previous studies on low-obliquity terra-planets which reported only one stable climate state for terra-planets with obliquities less than  $30^\circ$ .

In chapter 3, I showed that for zero obliquity, terra-planet can exist in two stable climate states: Hot and Dry (HD) and Cold and Wet (CW) states. Additionally, here I find for intermediate obliquities ( $5^\circ \leq \theta < 10^\circ$ ), a new stable climate state that I refer to as the 'Hot and Wet (HW) state in addition to the above mentioned HD and CW climate states. This new state has intense low-latitude precipitation like in the CW state however, the climate in the HW state is warmer than in the CW state. Also the snow cover in the HW state is limited to higher latitudes unlike in the CW state where it reaches up to  $40^\circ$  latitude. The extent of this HW state is limited. The stability of climate in this HW state is strongly governed by its strong greenhouse effect as a result of build up of huge amounts of water vapour in the low-latitude region of this state. The strong greenhouse warming is balanced by a large atmospheric heat transport to the higher latitudes which limits the snow cover to higher latitudes in this state. And, any slight decrease in greenhouse warming could lead to a slow transition to the CW state. There is no hysteresis between HW and CW states in the range of soil albedo values and obliquities considered in this chapter. This might allow the terra-planet to cycle between the HW and CW states with slight variations in soil surface albedo and obliquity.

Bistability (existence of both HD and CW states for the same boundary conditions), abrupt transitions from the HD to CW state and closed hysteretic behaviour is noticed also for non-zero obliquities. However, the width of the bi-stable region is significantly reduced with the increase in obliquity. And, bistability is completely lost at a larger obliquity (present-day Earth orbit value). I speculate the loss of bistability could be due to seasonal migration of rain bands into the low-latitude region with present-day obliquity. This would lead to seasonal rain and wet soils there. The wet soils due to their

long lasting memory can allow for continuous evaporation and precipitation in the low-latitude region. This probably destroys the HD state so that the planet is always self-stabilized in the CW state. Overall my findings suggest that it is more likely to find a terra-planet with a seasonal orbit in the CW state.



# Conclusions and Outlook

## 6.1 Conclusions

So far, studies on Earth-like terra-planets have reported only one stable climate state – a hot climate state with all the water on the planet trapped at the high latitudes. However, all these studies ignored the possible presence of an overland water recycling mechanism that can transfer fresh water from the high latitudes back to the low latitudes via rivers, glacier flows and subsurface flows on such dry planets. To investigate the influence of such an overland water recycling mechanism on the climate of Earth-like terra-planets, I performed a series of idealized climate model simulations of a homogenous land only planet with the general circulation model ICON. In these simulations, I assumed an unlimited subsurface reservoir of water to mimic the overland water recycling. The findings from these simulations are used to answer the research questions that were posed in *chapter 1.5*. The answers are as follows:

1. *What is the effect of water recycling on the climate of Earth-like terra-planets?*

The presence of an overland water recycling mechanism has a strong influence on the climate of Earth-like terra-planets. Terra-planets with an efficient water recycling can adopt two additional climate states beyond the well known hot and dry (HD) climate state reported in past studies – a cold climate state (CW state) with intense low latitude precipitation like on present-day Earth and a hot climate state (HW state for obliquities  $5^\circ$  and  $7^\circ$ ) with very intense low-latitude precipitation. The three terra-planet states differ drastically in their mean climate and atmospheric circulation patterns. The huge differences in climate between the terra-planet states are a result of completely different functioning of the hydrological cycle in each of the states.

2. *Can Earth-like terra-planets equipped with a water recycling mechanism exhibit multiple climate states for the same boundary conditions? Can abrupt transitions occur between different climate states?*

For perpetual equinox conditions, Terra-planet with an active water recycling mechanism exhibits bistability – both HD and CW climate states are stable below a threshold value of soil surface albedo of 0.15 while above that only the Cold and Wet state is stable. And, starting from the Hot and Dry state increasing soil surface albedo above the threshold causes an abrupt shift from the Hot and Dry state to the Cold and Wet state. This abrupt shift is associated with a cooling of about 35°C globally, which is in the order of the temperature difference between present day and the Snowball Earth state. Starting from the CW state and reducing the albedo down to zero does not shift back the terra-planet to the HD state indicating a hysteretic behaviour but no closed hysteresis.

Additionally, for obliquities 5° and 7°, when soil surface albedo in the HD state is increased above a critical threshold value, the terra-planet shifts abruptly from the HD state to a new climate state - warm and wet climate state. This abrupt shift is associated with a cooling of 20° C globally that is lower than the cooling associated with the terra-planet bifurcation from HD to CW state.

3. *Which processes are responsible for the stability of different climate states? What mechanisms lead to abrupt transitions between the climate states?*

The stability of the HD state is kept by the complete evaporation of rain drops which leads to enhance poleward moisture transport.

The transition from the HD state to the CW state is caused by the interactions between the evaporation of rain drops, the reverse circulation cell and poleward moisture transport. Diminishing of poleward winds is crucial for the initiation of rain in the low-latitude region and transition to the CW state.

4. *How does seasonal variability affect multistability and bifurcations on Earth-like terra-planets?*

The width of the bi-stable region on a terra-planet (range of soil surface albedo values for which both the HD and CW climate states are stable) is strongly reduced

with the increase in seasonal variability. Bistability is completely lost for present-day Earth's obliquity. Increase in seasonal variability also drastically reduces the threshold value of soil surface albedo at which the climate transitions from the HD state to the CW state. Overall a terra-planet with a non-zero obliquity is more likely to be found in the CW state.

On the whole, my findings provide a new perspective about the global hydrological cycle on water-limited planets.

## 6.2 Outlook

Although this study provides some new insights, it is only a first step towards understanding the possible hydro climate regimes for Earth-like planets. Many questions still remain that need to be addressed to gain a more comprehensive understanding about the water cycle and climate on such planets as well as terrestrial planets in general. In the following, I explore several future avenues of research.

### Representation of water cycle in the model

The novelty of this study is implementation of an effective overland water recycling mechanism on terra-planets. In the model used for this study, the water recycling is achieved by assuming an unlimited subsurface reservoir that is constantly refilled with water. And this water added to the subsurface equals the amount of water lost in the sink regions of the planet (regions where precipitation exceeds evaporation). For individual climate states under equilibrium condition, this assumption is valid since the amount of water lost in the sink regions remains constant. However, this is not completely true during the terra-planet transition case, because the total amount of water lost in the sink regions changes when climate transitions from Hot and Dry state to the Cold and Wet state. Accordingly, the rate at which the subsurface reservoir is refilled could be altered. As a consequence, water recycling rate would also change. This may have an effect on the occurrence of the bifurcation. This limitation is not taken into account in this study. A viable solution to keep the total water in the system also constant even during transition could be: implementing a closed water cycle in the model. The planet is provided with a fixed amount of water large enough to not dry out completely and let it evolve on its own. And check if a transition between the climate states could also be simulated with the closed water cycle setup.

## **Using thermodynamic analysis to study the abrupt bifurcation on terra-planets**

The usual indicator of a climate state – surface temperature is useful for defining an average state of climate, however it does not indicate whether the climate system is approaching a threshold point. Recent studies suggest that thermodynamic properties like Carnot efficiency, provide better information about the stability of the climate and hence are more useful in understanding climate tipping points like Snowball/Warm Earth transition (Lucarini et al., 2010; Boschi et la., 2013). Efficiency denotes how close/far the climate system from the equilibrium is. It is proportional to the differential heating resulting from meridional differences in solar insolation. Lower value of efficiency denotes that the negative feedbacks are very effective in dampening the differential heating and keeping the climate close to equilibrium. As the climate system approaches the bifurcation point, efficiency increases due to strengthening of the positive feedbacks which are not effective in dampening the differential heating indicating that the system is farther from the equilibrium state. At the bifurcation point, positive feedbacks overcome the negative feedbacks leading to the transition to a new climate state which can be seen by a sudden drop in efficiency. Therefore, these studies suggest that efficiency gives better information about tipping points than surface temperature. This approach can be applied to the terra-planet bifurcation to test whether similar deductions can be made as suggested by these recent thermodynamic studies. Preliminary analysis has already been performed in this direction.

## **Better representation of rain evaporation in climate models for studying warmer climates**

In my study, evaporation of falling rain drops was found to be an important process controlling the climate of terra-planets in the Hot and Dry state. My results suggest that the evaporation of rain drops can modify the vertical distribution of water vapour in the atmosphere and lead to sudden and large changes in the energetics of the atmosphere and circulation patterns. If this process is not correctly represented in models especially in studies concerning warmer climates or tropical dynamics, it may lead to large simulation biases. Currently general circulation models only include water vapour, cloud liquid water

and cloud ice as prognostic variables. This list could be extended to include rain drop size to more accurately simulate warmer climates.

### **Effect of other orbital parameters on the climate of terra-planets**

In this study, I only considered the effect of obliquity on the climate of terra-planets. However, other orbital parameters specifically eccentricity is also known to strongly influence seasonal variability of solar insolation received by the planet leading to drastic variations in climate on water-dominated terrestrial planets (Williams & Pollard 2002; Dressing et al. 2010; Linsenmeier et al. 2015). As an extension to my current study, simulations with non-zero eccentricity could be performed to gain a comprehensive understanding on the effects of seasonal variability of the climate of water-limited planets.

### **Range of possible climate states possible for terra-planets**

In this study, I have only considered a small range of physical properties (surface water availability, obliquity and surface albedo) that could affect the climate of terra-planets. However, a number of other factors could influence the climate of terra-planets/terrestrial planets in general (Forget and Leconte, 2014):

1. Physical characteristics like size, rotation, energy flux from the host star, type of star
2. Atmospheric composition which in turn depends on the water and carbon cycles.

Many of these factors are interdependent and a combination of all these factors could lead to a diverse range of possible climates for terrestrial planets. Examining the influence of each of these factors on the climate using climate models could help us to better understand the climate of terrestrial planets within our Solar System and to optimise future observation missions aimed at finding habitable exoplanets.



# Bibliography

- Abe, Y., Numaguti, A., Komatsu, G., and Kobayashi, Y.: Four climate regimes on a land planet with wet surface: Effects of obliquity change and implications for ancient Mars, *Icarus*, 178, 27–39, <https://doi.org/10.1016/j.icarus.2005.03.009>, 2005.
- Abe, Y., Abe-Ouchi, A., Sleep, N. H., and Zahnle, K. J.: Habitable Zone Limits for Dry Planets, *Astrobiology*, 11, 443–460, <https://doi.org/10.1089/ast.2010.0545>, 2011.
- Aleina, F. C., Baudena, M., D'Andrea, F., and Provenzale, A.: Multiple equilibria on planet dune: Climate-vegetation dynamics on a sandy planet, *Tellus B*, 65, 17662, <https://doi.org/10.3402/tellusb.v65i0.17662>, 2013.
- Baudena, M, Boni, G, Ferraris, L, von Hardenberg, J and Provenzale, A.: Vegetation response to rainfall intermittency in drylands: Results from a simple ecohydrological box model. *Adv. Water Res.* 30(5): 1320–1328. DOI: 10.3402/tellusb.v65i0.17662, 2007
- Baudena, M, D'Andrea, F and Provenzale, A.: A model for soil-vegetation-atmosphere interactions in water-limited ecosystems. *Water Resour. Res.* 44(12): 1–9. DOI: 10.3402/tellusb.v65i0.17662, 2008.
- Baudena, M and Provenzale, A.: Rainfall intermittency and vegetation feedbacks in drylands. *Hydrol. Earth Syst. Sc.* 12(2): 679–689. DOI: 10.3402/tellusb.v65i0.17662, 2008
- Becker, T. and Stevens, B.: Climate and climate sensitivity to changing CO<sub>2</sub> on an idealized land planet, *J. Adv. Model. Earth Syst.*, 6, 1205–1223, <https://doi.org/10.1002/2014MS000369>, 2014.
- Brovkin V, Claussen M, Petoukhov V. On the stability of the atmosphere-vegetation system in the Sahara/Sahel region. *J. Geophys. Res.*, 103: 31, 613–631. [10.3402/tellusb.v65i0.17662](https://doi.org/10.3402/tellusb.v65i0.17662), 1998.
- Brubaker, K., and D. Entekhabi: An analytic approach to modeling land atmosphere interaction: 1. Construct and equilibrium behavior. *Water Resour. Res.*, 31, 619–632, doi:10.1029/94WR01772, 1995.
- Boschi, R., Lucarini, V., and Pascale, S.: Bistability of the climate around the habitable zone: A thermodynamic investigation, *Icarus*, 226, 1724–1742, <https://doi.org/10.1016/j.icarus.2013.03.017>, 2013.
- Budyko, M. I.: The effect of solar radiation variations on the climate of the Earth, *Tellus*, 21, 611–619, <https://doi.org/10.3402/tellusa.v21i5.10109>, 1969.
- Caballero, R., Pierrehumbert, R. T., and Mitchell, J. L.: Axisymmetric, nearly inviscid circulations in non-condensing radiative-convective atmospheres, *Q. J. Roy. Meteorol. Soc.*, 134, 1269–1285, <https://doi.org/10.1002/qj.271>, 2008.

Dressing C.D., Spiegel D.S., Scharf C.A., Menou K., Raymond S.N.: **Habitable climates: the influence of eccentricity**, *Astrophys. J.*, 721 (2), p. 1295, 2010.

Entekhabi, D., and K. Brubaker,: An analytic approach to modeling land-atmosphere interaction: 2. Stochastic formulation. *Water Resour. Res.*, 31, 633–643, doi:10.1029/94WR01773, 1995.

—, I. Rodriguez-Iturbe, and R. L. Bras,: Variability in largescale water balance with land surface-atmosphere interaction. *J. Climate*, 5, 798–813, doi:10.1175/1520-0442(1992)005,0798: VILSWB.2.0.CO;2, 1992.

Fairchild, I. J. and Kennedy, M. J.: Neoproterozoic glaciation in the Earth System, *J. Geol. Soc. Lond.*, 164, 895–921, <https://doi.org/10.1144/0016-76492006-191>, 2007.

Forget. F and Leconte. J.: Possible climates on terrestrial exoplanets, *Phil. Trans. R. Soc. A* **372**, 20130084, [doi:10.1098/rsta.2013.0084](https://doi.org/10.1098/rsta.2013.0084), 2014.

Hagemann, S. and Stacke, T.: Impact of the soil hydrology scheme on simulated soil moisture memory, *Clim. Dynam.*, 44, 1731–1750, <https://doi.org/10.1007/s00382-014-2221-6>, 2015.

Hart, M. H.: The evolution of the atmosphere of the earth, *Icarus*, 33, 23–39, [https://doi.org/10.1016/0019-1035\(78\)90021-0](https://doi.org/10.1016/0019-1035(78)90021-0), 1978.

Held, I. M. and Hou, A. Y.: Nonlinear Axially Symmetric Circulations in a Nearly Inviscid Atmosphere, *J. Atmos. Sci.*, 37, 515–533, [https://doi.org/10.1175/1520-0469\(1980\)037<0515:NASCIA>2.0.CO;2](https://doi.org/10.1175/1520-0469(1980)037<0515:NASCIA>2.0.CO;2), 1980.

Herbert, F.: *Dune*, Chilton Books, Philadelphia, 1965.

Hoffman, P. F. and Schrag, D. P.: The snowball Earth hypothesis: testing the limits of global change, *Terra Nova*, 14, 129–214, <https://doi.org/10.1046/j.1365-3121.2002.00408.x>, 2002.

Iacono, M. J., Delamere, J. S., Mlawer, E. J., Shephard, M. W., Clough, S. A., and Collins, W. D.: Radiative forcing by long-lived greenhouse gases: Calculations with the AER radiative transfer models, *J. Geophys. Res.*, 113, D13103, <https://doi.org/10.1029/2008JD009944>, 2008.

Kasting, J. F., Whitmire, D. P., and Reynolds, R. T.: Habitable Zones around Main Sequence Stars, *Icarus*, 1, 108–128, <https://doi.org/10.1006/icar.1993.1010>, 1993.

Kilic, C., Raible, C. C., and Stocker, T. F.: Multiple Climate States of Habitable Exoplanets: The Role of Obliquity and Irradiance, *The Astrophysical Journal*, 844, 147, <https://doi.org/10.3847/1538-4357/aa7a03>, 2017.

Kopparapu, R. K., Ramirez, R. M., Schottel Kotte, J., Kasting, J. F., Domagal-Goldman, S., and Eymet, V.: Habitable zones around main-sequence stars: dependence on planetary mass, *Astrophys. J.*, 787, L29, <https://doi.org/10.1088/2041-8205/787/2/L29>, 2014.

Leconte, J., Forget, F., Charnay, B., Wordsworth, R., Selsis, F., Millour, E., and Spiga, A.: 3D climate modeling of close-in land planets: Circulation patterns, climate moist bistability,

- and habitability, *Astron. Astrophys.*, 554, A69, <https://doi.org/10.1051/0004-6361/201321042>, 2013.
- Linsenmeier, M., Pascale, S., and Lucarini, V.: Climate of Earth-like planets with high obliquity and eccentric orbits: Implications for habitability conditions, *Planet. Space Sci.*, 105, 43–59, <https://doi.org/10.1016/j.pss.2014.11.003>, 2015.
- Lohmann, U. and Roeckner, E.: Design and performance of a new cloud microphysics scheme developed for the ECHAM general circulation model, *Clim. Dynam.*, 12, 557–572, <https://doi.org/10.1007/BF00207939>, 1996.
- Lucarini, V., Fraedrich, K., and Lunkeit, F.: Thermodynamic analysis of snowball earth hysteresis experiment: Efficiency, entropy production and irreversibility, *Quarterly Journal of the Royal Meteorological Society*, 136, 2–11, <https://doi.org/10.1002/qj.543>, 2010b.
- Lucarini, V., Pascale, S., Boschi, R., Kirk, E., and Iro, N.: Habitability and multistability in earth-like planets, *Astron. Nachrichten*, 334, 576–588, <https://doi.org/10.1002/asna.201311903>, 2013.
- Marotzke, J. and Botzet, M.: Present-day and ice-covered equilibrium states in a comprehensive climate model, *Geophys. Res. Lett.*, 34, L16704, <https://doi.org/10.1029/2006GL028880>, 2007.
- Micheels, A. and Montenari, M.: A snowball Earth versus a slushball Earth: Results from Neoproterozoic climate modeling sensitivity experiments, *Geosphere*, 4, 401–410, <https://doi.org/10.1130/GES00098.1>, 2008.
- Mitchell, J. L.: The drying of Titan's dunes: Titan's methane hydrology and its impact on atmospheric circulation, *J. Geophys. Res.-Planets*, 113, E08015, <https://doi.org/10.1029/2007JE003017>, 2008.
- Mitchell, J. L., Pierrehumbert, R. T., Frierson, D. M. W., and Caballero, R.: The dynamics behind Titan's methane clouds, *P. Natl. Acad. Sci. USA*, 103, 421–426, <https://doi.org/10.1073/pnas.0605074103>, 2006.
- Mitchell, J. L., Pierrehumbert, R. T., Frierson, D. M. W., and Caballero, R.: The impact of methane thermodynamics on seasonal convection and circulation in a model Titan atmosphere, *Icarus*, 203, 250–264, <https://doi.org/10.1016/j.icarus.2009.03.043>, 2009.
- Mlawer, E. J., Taubman, S. J., Brown, P. D., Iacono, M. J., and Clough, S. A.: Radiative transfer for inhomogeneous atmospheres: RRTM, a validated correlated-*k* model for the longwave, *J. Geophys. Res.-Atmos.*, 102, 16663–16682, <https://doi.org/10.1029/97JD00237>, 1997.
- Nolan, D. S., Zhang, C., and Chen, S.: Dynamics of the Shallow Meridional Circulation around Intertropical Convergence Zones, *J. Atmos. Sci.*, 64, 2262–2285, <https://doi.org/10.1175/JAS3964.1>, 2007.
- Nordeng, T. E.: Extended versions of the convective parametrization scheme at ECMWF and their impact on the mean and transient activity of the model in the tropics, ECMWF Tech. Memo. 206, Eur. Cent. for Medium-Range Weather Forecasts, Reading, UK, 1994.

- Pierrehumbert, R. T.: Climate dynamics of a hard snowball Earth, *J. Geophys. Res.-Atmos.*, 110, D01111, <https://doi.org/10.1029/2004JD005162>, 2005.
- Pierrehumbert, R. T., Abbot, D. S., Voigt, A., and Koll, D.: Climate of the Neoproterozoic, *Annu. Rev. Earth Planet. Sci.*, 39, 417–460, <https://doi.org/10.1146/annurev-earth-040809-152447>, 2011.
- Popp M., Schmidt H., Marotzke J.: Transition to a Moist Greenhouse with CO<sub>2</sub> and solar forcing, *Nature Communications*, 2041-1723, doi:10.1038/ncomms10627, 2016.
- Rochetin, N., Lintner, B. R., Findell, K. L., Sobel, A. H., and Gentine, P.: Radiative-convective equilibrium over a land surface, *J. Climate*, 27, 8611–8629, <https://doi.org/10.1175/JCLI-D-13-00654.1>, 2014.
- Roeckner, E., Brokopf, R., Esch, M., Giorgetta, M., Hagemann, S., Kornblueh, L., Manzini, E., Schlese, U. and Schulzweida, U.: The atmospheric general circulation model ECHAM 5. PART II: Sensitivity of the simulated climate to horizontal and vertical resolution, *J. Climate*, 19, 3771–3791, <https://doi.org/10.1175/JCLI3824.1>, 2004.
- Rodriguez-Iturbe, I., D. Entekhabi, and R. L. Bras,: Nonlinear dynamics of soil moisture at climate scales. 1. Stochastic analysis. *Water Resour. Res.*, 27, 1899–1906, doi:10.1029/91WR01035, 1991a
- , ——, J.-S. Lee, and R. L. Bras,: Nonlinear dynamics of soil moisture at climate scales. 2. Chaotic analysis. *Water Resour. Res.*, 27, 1907–1915, doi:10.1029/91WR01036, 1991b.
- Scheffer, M., Carpenter, S., Foley, J. a., Folke, C., and Walker, B.: Catastrophic shifts in ecosystems, *Nature*, **413**( 6856), 591– 596, doi:[10.1038/35098000](https://doi.org/10.1038/35098000), 2001.
- Schulze-Makuch, D., Méndez, A., Fairén, A. G., von Paris, P., Turse, C., Boyer, G., Davila, A. F., de António, M. R. S., Catling, D., and Irwin, L. N.: A Two-Tiered Approach to Assessing the Habitability of Exoplanets, *Astrobiology*, 11, 1041–1052, <https://doi.org/10.1089/ast.2010.0592>, 2011.
- Sellers, W. D.: A global climatic model based on the energy balance of the earth-atmosphere system, *J. Appl. Meteorol.*, 476, 1373–1387, [https://doi.org/10.1175/1520-0450\(1969\)008<0392:AGCMBO>2.0.CO;2](https://doi.org/10.1175/1520-0450(1969)008<0392:AGCMBO>2.0.CO;2), 1969.
- Stevens, B., Giorgetta, M., Esch, M., Mauritsen, T., Crueger, T., Rast, S., Salzmann, M., Schmidt, H., Bader, J., Block, K., Brokopf, R., Fast, I., Kinne, S., Kornblueh, L., Lohmann, U., Pincus, R., Reichler, T., and Roeckner, E.: Atmospheric component of the MPI-M earth system model: ECHAM6, *J. Adv. Model. Earth Syst.*, 5, 146–172, <https://doi.org/10.1002/jame.20015>, 2013.
- Suni, T., Guenther, A., Hansson, H.C., Kulmala, M., Andreae, M.O., Arneth, A., Artaxo, P., Blyth, E., Brus, M., Ganzeveld, L., Kabat, P., De Noblet-Ducoudré, N., Reichstein, M., Reissell, A., Rosenfeld, D., Seneviratne, S: The significance of land-atmosphere interactions in the Earth system – ILEAPS achievements and perspectives. *Anthropocene* 12, 69–84, <https://doi.org/10.1016/j.ancene.2015.12.001>, 2015

- Tiedtke, M.: A Comprehensive Mass Flux Scheme for Cumulus Parameterization in Large-Scale Models, *Mon. Weather Rev.*, 117, 1779–1800, [https://doi.org/10.1175/1520-0493\(1989\)117<1779:ACMFSF>2.0.CO;2](https://doi.org/10.1175/1520-0493(1989)117<1779:ACMFSF>2.0.CO;2), 1989.
- Voigt, A. and Marotzke, J.: The transition from the present-day climate to a modern Snowball Earth, *Clim. Dynam.*, 35, 887–905, <https://doi.org/10.1007/s00382-009-0633-5>, 2010.
- Voigt, A., Abbot, D. S., Pierrehumbert, R. T., and Marotzke, J.: Initiation of a Marinoan Snowball Earth in a state-of-the-art atmosphere–ocean general circulation model, *Clim. Past*, 7, 249–263, <https://doi.org/10.5194/cp-7-249-2011>, 2011.
- Williams D.M., Pollard. D.: Earth-like worlds on eccentric orbits: excursions beyond the habitable zone, *Int. J. Astrobiol.*, 1, pp. 61-69, 2002.
- Wolf, E. T. & Toon, O. Delayed onset of runaway and moist greenhouse climates for earth. *Geophys. Res. Lett.* **41**, 167–172 (2014).
- Zängl, G., Reinert, D., Rípodas, P., and Baldauf, M.: The ICON (ICOsahedral Non-hydrostatic) modelling framework of DWD and MPI-M: Description of the non-hydrostatic dynamical core, *Q. J. Roy. Meteorol. Soc.*, 141, 563–579, <https://doi.org/10.1002/qj.2378>, 2015.
- Zeng, N.: Enhancement of interdecadal climate variability in the Sahel by vegetation interaction. *286(5444): 1537–1540*. DOI: 10.3402/tellusb.v65i0.17662, 1999.
- Zhang, C., McGauley, M., and Bond, N. A.: Shallow meridional circulation in the tropical eastern Pacific, *J. Climate*, 17, 133–139, [https://doi.org/10.1175/1520-0442\(2004\)017<0133:SMCITT>2.0.CO;2](https://doi.org/10.1175/1520-0442(2004)017<0133:SMCITT>2.0.CO;2), 2004.
- Zhang, C., Nolan, D. S., Thorncroft, C. D., and Nguyen, H.: Shallow meridional circulations in the tropical atmosphere, *J. Climate*, 21, 3453–3470, <https://doi.org/10.1175/2007JCLI1870.1>, 2008.
- Zsom, A., Seager, S., and De Wit, J.: Toward the minimum inner edge distance of the habitable zone, *Astrophys. J.*, 778, 109, <https://doi.org/10.1088/0004-637X/778/2/109>, 2013.

# Acknowledgements

First of all, I would like to thank my co-supervisor Martin Claussen for pitching me this fantastic and fun idea for the PhD thesis. I am very grateful to my principle advisor, Christian Reick and co-supervisors, Thomas Raddatz and Martin Claussen for their tremendous support, lots of encouragement and great guidance through out my PhD. This thesis would not be possible without them. I always loved our very long, fun, brain storming sessions. Special thanks to Thomas for proof reading most parts of this thesis and pushing me to submit the thesis.

Many thanks to Reiner Schnur and Rainer Schneck for helping me with the model and the whole Land department. I enjoyed being part of this department. I am grateful to Juergen Bader for sharing office with me and helping me in translating the abstract.

Thanks to Vivi, Sylvia, Johannes, Cathy, Elnaz, Gui, Pinhsin, Hao-wei, Suman, Doro, Rohit and Jörg for the fun lunch times. And Josiane and Tobias for constant help regarding ICON.

Special thanks to Antje Weitz, Cornelia Kampmann, Michaela Born, and Wiebke Böhm for making everything easier at MPI, settling down in Hamburg and administrative issues.

I am grateful to Geetha, Sanjeev, Anjany, Harsha and Madhu for their constant love and support despite being so far in a different continent.

Most of all I would like to thank my family, Mom, dad, Viky and Gayi for their love and encouragement for everything I do in my life and supporting my decision to move to a different continent for pursuing my dreams.

## VERSICHERUNG AN EIDES STATT

### Declaration of oath

Hiermit versichere ich an Eides statt, dass ich die vorliegende Dissertation mit dem Titel: Multiple climate states and bifurcations on Earth-like terra-planets selbstständig verfasst und keine anderen als die angegebenen Hilfsmittel – insbesondere keine im Quellenverzeichnis nicht benannten Internet-Quellen – benutzt habe. Alle Stellen, die wörtlich oder sinngemäß aus Veröffentlichungen entnommen wurden, sind als solche kenntlich gemacht. Ich versichere weiterhin, dass ich die Dissertation oder Teile davon vorher weder im In- noch im Ausland in einem anderen Prüfungsverfahren eingereicht habe und die eingereichte schriftliche Fassung der auf dem elektronischen Speichermedium entspricht.

Hamburg, den 03.04.2019

Sirisha Kalidindi



## Hinweis / Reference

Die gesamten Veröffentlichungen in der Publikationsreihe des MPI-M  
„Berichte zur Erdsystemforschung / Reports on Earth System Science“,  
ISSN 1614-1199

sind über die Internetseiten des Max-Planck-Instituts für Meteorologie erhältlich:  
**<http://www.mpimet.mpg.de/wissenschaft/publikationen.html>**

*All the publications in the series of the MPI -M  
„Berichte zur Erdsystemforschung / Reports on Earth System Science“,  
ISSN 1614-1199*

*are available on the website of the Max Planck Institute for Meteorology:  
**<http://www.mpimet.mpg.de/wissenschaft/publikationen.html>***





